

**ARDHI UNIVERSITY**



**ANALYZING THE IMPACT OF CLIMATE VARIABILITY ON  
VEGETATION COVER USING EARTH OBSERVATION DATA**

**A Case Study of Katuma Sub-Basin**

**LAURA JOSEPHAT MBOYA**

**BSc. Geoinformatics**

**Dissertation**

**Ardhi University, Dar es Salaam**

**July 2023**

ANALYZING THE IMPACT OF CLIMATE VARIABILITY ON VEGETATION COVER  
USING EARTH OBSERVATION DATA

A Case Study of Katuma Sub-Basin

Mboya, Laura J

A Dissertation Submitted to the Department of Geospatial Sciences and Technology in  
Partially Fulfilment of the Requirements for the Award of Science in Geoinformatics  
(BSc. GI) of Ardhi University

## **CERTIFICATION**

The undersigned certify that they have read and hereby recommended for acceptance by the Ardhi University a dissertation that titled “**Analyzing the Impact of Climate Variability on Vegetation Cover Using Earth Observation Data, A Case Study of Katuma Sub-Basin.**”  
In fulfilment of the requirements for the Bachelor of Science degree in Geoinformatics.

.....  
**Dr. Zakaria Robert Ngereja**

(Main Supervisor)

Date.....

.....  
**Mr. Michael Mavura**

(Second Supervisor)

Date.....

## **DECLARATION AND COPYRIGHT**

I, Mboya Laura J, hereby declare that the content of this work were the results of my own findings and study and to the best of my knowledge. Any reference to work done by any other person or institution or any other material obtained from other sources have been dully cited and referenced. I certify that the research report has not been presented or published elsewhere.

.....

**Mboya, Laura J**

22733/T.2019

(Candidate)

Copyright ©1999 This dissertation is the copyright material presented under Berne convention, the copyright act of 1999 and other international and national enactments, in that belief, on intellectual property. It may not be reproduced by any means, in full or in part, except for short extracts in fair dealing; for research or private study, critical scholarly review or discourse with an acknowledgement, without the written permission of the directorate of undergraduate studies, on behalf of both the author and Ardhi University.

.

## **ACKNOWLEDGEMENTS**

I would like to express my sincere gratitude to Almighty God for granting me knowledge and good health throughout my dissertation. I am thankful for the strength, health, knowledge, and wisdom to complete this study.

I extend my heartfelt appreciation to my supervisors, Dr. Zakaria Robert Ngereja and Mr. Michael Mavura, together with Dr. Dorothea Deus for their exceptional and unwavering support, kindness, understanding, and encouragement throughout this research. I am grateful to the members of the Geospatial Science and Technology Department (DGST) for their invaluable support, which significantly influenced the shaping of my methods and the critique of my results.

Lastly, but not least, I would like to thank my friends Jones Kamwenda, Mbwana Said, Clinton Lyimo, Salvina Mwumbe, Elizabeth Kassase, Elifaraja Mazengo, Gadiel Simon, Elizabeth Mwanda, and Daria Lazaro. Your contributions to this research sincerely appreciated and gratefully acknowledged. This appreciation extends to all of my colleagues and anyone else who contributed in any way to making this research successful. May God's blessings be manifested in all of you

## **DEDICATION**

*To my parents, Josephat Mboya and Dora Mongi, together with my siblings Irene, John, and Elizabeth, as well as my close friends. Their prayers, love, support, and encouragement have made it possible for me to reach this stage. May God bless you.*

## ABSTRACT

The research aimed to investigate the relationship between climate variability and vegetation cover dynamics in the Katuma sub-basin. An integrated approach of data acquisition, preparation, processing, and analysis was employed, utilizing Landsat 7 and 8 imageries for land cover analysis, Terra climate dataset for temperature and rainfall trends, and MODIS data for the Normalized Difference Vegetation Index (NDVI).

The analysis revealed significant changes in vegetation cover over time, as indicated by the generated land cover maps. The NDVI time series analysis showed a positive trend of 0.00033, although it was not statistically significant at 0.47. However, the NDVI distribution map indicated varying vegetation health levels, with lower vegetation health observed in 2007 and higher vegetation health in 2010.

Positive temperature trends were observed, between a maximum temperature trend of 0.01109 and a minimum temperature trend of 0.01323. Precipitation exhibited a positive trend of 4.871, and these trends were statistically significant at 0.00201, 0.0497 and 0.0275 respectively. Correlation analysis demonstrated a significant positive correlation between NDVI and precipitation, with a correlation coefficient of 0.68, which was statistically significant at 0.00063. Negative correlations were found between vegetation cover and maximum temperature (-0.6847) as well as minimum temperature (-0.6164). Additionally, a positive correlation of 0.5077 was observed between vegetation cover and precipitation.

In conclusion, this integrated study utilizing Landsat, terra climate dataset and MODIS data provides valuable insights into the relationship between climate variability, land cover dynamics, and vegetation cover in the Katuma sub-basin. The analysis revealed significant changes in vegetation cover, positive temperature trends, and significant correlations between NDVI and precipitation, emphasizing the importance of adequate rainfall for a healthy vegetation ecosystem. The correlations between vegetation cover and climatic parameters further contribute to our understanding of the mechanisms driving vegetation dynamics in response to climate variability. The NDVI time series analysis showed a positive trend, although not statistically significant, while the NDVI distribution map indicated varying vegetation health levels between different years

**Keywords:** Climate variability, vegetation cover dynamics, Katuma sub-basin, NDVI, Landsat, Terra climate dataset, MODIS, temperature trends, precipitation trends, correlation analysis, integrated approach.

## TABLE OF CONTENTS

<b>CERTIFICATION</b> .....	ii
<b>DECLARATION AND COPYRIGHT</b> .....	iii
<b>ACKNOWLEDGEMENTS</b> .....	iv
<b>DEDICATION</b> .....	v
<b>ABSTRACT</b> .....	vi
<b>LIST OF FIGURES</b> .....	x
<b>LIST OF TABLES</b> .....	xi
<b>CHAPTER ONE</b> .....	1
<b>INTRODUCTION</b> .....	1
1. 1 Background.....	1
1.2 Statement of the research problem.....	2
1.3 Objectives .....	2
1.3.1 Main Objective.....	2
1.3.2 Specific Objectives .....	2
1.4 Research Questions .....	2
1.5 Significance of the research .....	3
1.6 Beneficiaries .....	3
1.7 Description of the Study area.....	3
1.8 Dissertation structure .....	4
<b>CHAPTER TWO</b> .....	6
<b>LITERATURE REVIEW</b> .....	6
2.1 Overview .....	6
2.2 Remote sensing in relation to vegetation cover and climate.....	6
2.3 Spectral indices on vegetation .....	8
2.4 Climate variability .....	8
2.5 Raster trend analysis .....	9



2.6 Correlation analysis .....	9
2.7 Land Cover Mapping .....	11
2.7.1 Image classification .....	11
2.7.2 Classification schemes .....	12
2.7.3 Separability analysis .....	13
2.7.4 Classification algorithms .....	14
2.7.5 Accuracy assessment .....	14
<b>CHAPTER THREE .....</b>	<b>17</b>
<b>METHODOLOGY .....</b>	<b>17</b>
3.1 Overview .....	17
3.2 Data Acquisition.....	18
3.2.1 Landsat images.....	18
3.2.2 MODIS images .....	19
3.2.3 TerraClimate Data.....	19
3.3 Software used.....	20
3.4 Data preparation.....	20
3.4.1 Landsat images.....	20
3.4.2 Layer stacking .....	21
3.4.3 Image re-projection.....	21
3.4.4 Mosaicking.....	21
3.4.5 DE stripping .....	21
3.4.6 Image subset.....	21
3.4.7 Terra climate data .....	21
3.4.8 MODIS data .....	22
3.5 Data processing.....	22
3.5.1 Normalized Differenced Vegetation Index (NDVI) .....	22
3.5.2 Regression analysis.....	22

3.5.3 Classification.....	22
3.6 Data analysis .....	23
3.6.1 Mann-Kendall test.....	23
3.6.2 Correlation analysis .....	23
<b>CHAPTER FOUR.....</b>	<b>25</b>
<b>RESULTS AND DISCUSSION .....</b>	<b>25</b>
4.1 Overview .....	25
4.2 Normalized Differenced Vegetation Index (NDVI) .....	25
4.3 Climate change.....	27
4.3.1 Annual Maximum Temperature trend .....	27
4.3.2 Annual minimum temperature trend .....	28
4.3.3 Overall temperature trend .....	29
4.3.4 Annual rainfall trend .....	30
4.4 Mann Kendall results .....	31
4.5 Correlation results .....	32
4.6 land cover.....	33
4.6.1 Accuracy assessment .....	38
4.6.2 Separability analysis .....	39
4.6.3 Quantification of the land cover .....	40
4.6.4 Correlation analysis .....	42
4.6.5 Land cover change .....	43
4.7 Discussion .....	49
<b>CHAPTER FIVE .....</b>	<b>51</b>
<b>CONCLUSION AND RECOMMENDATION .....</b>	<b>51</b>
5.1 Conclusion .....	51
5.2 Recommendation .....	52
<b>REFERENCE .....</b>	<b>53</b>

## LIST OF FIGURES

Figure 1.1: Location of the study area .....	4
Figure 3.2: Methodology work flow diagram of the research .....	15
Figure 4.1: NDVI distribution map of Katuma Sub-Basin (2000-2020) .....	26
Figure 4.2: NDVI time series of Katuma Sub-Basin 2000-2020.....	27
Figure 4.3: The annual maximum temperature trend of Katuma Sub-Basin 2000-2020.....	28
Figure 4.4: The annual minimum temperature trend of the Katuma Sub-Basin 2000-2020 ..	29
Figure 4.5: The overall maximum and minimum temperature trend of Katuma Sub-Basin 2000-2020.....	30
Figure 4.6: The annual rainfall trend of Katuma Sub-Basin 2000-2020 .....	31
Figure 4.7: Correlation plot between NDVI and rainfall of Katuma Sub-Basin 2000-2020...	33
Figure 4.8: Land cover maps on vegetation cover in the Katuma Sub-Basin of 2000 .....	35
Figure 4.9: Land cover map on vegetation cover in Katuma Sub-Basin of 2010.....	36
Figure 4.10: Land cover map on vegetation cover in Katuma Sub-Basin 2020.....	37
Figure 4.11: Showing the graphical representation of the land cover classes. ....	42
Figure 4.12: Change detection map showing changes in vegetation cover from 2000 to 2010.....	44
Figure 4.13: Graph showing area change of vegetation cover in Katuma sub basin (2000-2013) .....	45
Figure 4.14: Change detection map showing changes in vegetation cover from 2010 to 2020.....	46
Figure 4.15: Graph showing area change of vegetation cover in Katuma Sub-Basin (2010-2020) .....	47
Figure 4.16: Change detection map showing change in vegetation cover from 2000-2020....	48
Figure 4.17: Graph showing area change of forest cover in Katuma Sub-Basin (2000-2020) 49	

## LIST OF TABLES

Table 2.1: A summary of LULC classes as per Land-Based Classification Standard (Jensen, 2015) .....	12
Table 2.2: Four levels of LBCS (Jensen, 2015).....	13
Table 3.1:Landsat data acquired .....	18
Table 3.2: Table showing attributes of MOD09A1 .....	19
Table 3.3: Summary of Terra climate data characteristics and sources.....	20
Table 3.4: Software used in the study .....	20
Table 4.1: Mann Kendall result .....	32
Table 4.2: Confusion matrix for the classified image of 2000 .....	38
Table 4.3: Confusion matrix of the classified image of 2013.....	39
Table 4.4: Confusion matrix of the classified image of 2020.....	39
Table 4.5: Separability table .....	40
Table 4.6: Showing the percentage of the land cover classes.....	41
Table 4.7: Showing the relationship between temperature, rainfall and vegetation cover for the year 2000, 2010 and 2020 respectively.....	42
Table 4.8: Showing the correlation values of the datasets.....	43

## CHAPTER ONE

### INTRODUCTION

#### 1. 1 Background

Climate variability refers to the variation in the mean state and other climate statistics on temporal and spatial scales beyond those of individual weather event. The shifts of the temperature and weather patterns may be natural such as through variation in the solar system or artificial such as the anthropogenic activities (Cloern et al., 2016). Increase in the human population rises competition in survival since, more people requires more food and more water thus increasing the conflicts of people in down streams, and up streams areas and between people and the nature in much of the semi-arid East African countries (Mbonile, 2005). A sustainable water supply requires healthy watersheds and water resources. Healthy of the water resources directly affects the day-to-day ongoing human activities (Tzanakakis, 2020). The Inter-Governmental panel on climate change the world is set to reach the 1.5 degree centigrade threshold above the pre-industrial level within the next two decades and the only most drastic cuts in carbon emission from now would help prevent the environmental disasters. The changes in climate such as rising of maximum and minimum temperature, increased variability of rainfall and the increased frequency and severity of extreme events reported in the case of Tanzania (Agrawala et al., 2003). Causes of water crisis are many such as erosion overgrazing of cattle leading to desertification in the dry seasons, illegal wears in rivers last but not the least is illegal irrigation channels providing no return flow to the rivers (Mnaya et al., 2021).

Tanzania divided into nine administrative basins under the Tanzania Ministry of water, which generally follow Natural River or lake basins boundaries (Seeteram et al., 2019). The nine administrative basins are Pangani basins, Wami-Ruvu basins, Rufiji basins, Ruvuma and southern coast basins, internal drainage basins, Lake Rukwa basins, Lake Tanganyika basins and Lake Victoria basins. Each of these basins made of the following characteristics: the drainage basin, catchments area, watershed, source, confluence, tributaries and the mouth.

Katuma sub basin consists of the Mpanda, Msanginya and Katuma rivers and feeds into the lake Rukwa basin in the southwestern Tanzania (International, 2016). The catchment is not only for the basin and the downstream communities but also for the survival of the Katavi National park and its surrounding ecosystem. The local says, “Without Katuma River there will be no Katavi National Park” often says it. The main reasons of the reduced river flow were the illegal abstraction by the smallholder farmers and irregular and reduced rainfall due to climate

change. Due to vegetation richness more especially the Miombo ecosystem and grasslands in Katuma sub-basin (Munishi et al., 2011). It makes it an ideal study area for the research

## **1.2 Statement of the research problem**

The Katuma sub-basin in Tanzania grapples with a critical knowledge gap regarding the intricate interplay between climate variability and vegetation dynamics. This limited understanding hinders a comprehensive assessment of climate's impact on vegetation cover over time. To bridge this gap, this study aims to investigate the effects of climate variability on vegetation cover using earth observation data. By unraveling the complex relationship between climatic shifts and vegetation dynamics, this research seeks to provide insights crucial for informed decision-making, sustainable land management, and ecological conservation in the Katuma sub-basin.

## **1.3 Objectives**

### **1.3.1 Main Objective**

The primary goal of this research is Analyzing the impact of climate variability on vegetation cover in the Katuma sub basin using earth observation data from 2000-2020.

### **1.3.2 Specific Objectives**

This research seeks to accomplish the following specific objectives:

- i. Assessing the land cover dynamics in the Katuma sub-basin
- ii. Quantifying temperature and rainfall trends of the vegetation cover
- iii. Investigating the correlation between the time series of Normalized Difference Vegetation Index (NDVI) and precipitation, as well as exploring the correlation between quantified vegetation values and climatic parameters.

## **1.4 Research Questions**

This research seeks to address three key research questions within the context of the Katuma sub-basin's ecosystem from 2000 to 2020:

- i. What are the land cover changes observed from 2000 to 2020?
- ii. How have temperature and rainfall patterns influenced the vegetation cover from 2000 to 2020?
- iii. What is the relationship between NDVI and precipitation, and how do they correlate with quantified vegetation values and other climatic parameters in the Katuma sub-basin from 2000 to 2020?

### **1.5 Significance of the research**

The significance of this research is to provide information in the analyzing how climate variability can have its impacts on vegetation cover in the Katuma sub basin providing a clear understanding on the issue of climate variability impact on the vegetation cover. It will be of more usefulness in the management and conservation of the water resources for the water supply to wildlife and other activities for people living proximity to the park. Lastly, enables environment conservationists to take the proactive actions and incentives to tackle the vegetation variation in the sub-basins and basins as whole.

### **1.6 Beneficiaries**

Beneficiaries these are individuals, organizations, or institutions that will benefit from the research topic. The following are the beneficiaries of the research outputs.

#### **i. Researchers**

This study gives the ability to obtain accurate and reliable information on the state of the vegetation cover over time such as deforestation, forest degradation and forest regeneration. Which can help researchers understand the impact of climate variability on forest cover.

#### **ii. TANAPA**

This study brings the ability to develop effective conservation strategies and management plans for the park's resources, particularly its vegetation cover and water supply. This is by obtaining reliable information on the state of forest cover and water resources in the region. TANAPA can identify areas of concern and prioritize conservation efforts accordingly.

#### **iii. Decision, policy makers and local communities**

The study provides the decision makers with insights into the impacts of climate variability on vegetation cover, which can inform policies related to deforestation, forest degradation and forest restoration efforts. Additionally, provides the local communities with the information and tools they need to manage their natural resources sustainably adapt to climate change and improve their livelihoods.

### **1.7 Description of the Study area**

Lake Rukwa basin is located in the south- western part of Tanzania and is part of the East African Rift Valley with Lake Tanganyika on the northwest and Lake Nyasa on the southwest. Lake Rukwa has six sub basins with a total area of 88,000 square kilometer. The six sub basin present in Lake Rukwa basins are Katuma, Momba, Rungwa, Songwe, Lwiche and Muze.

The Katuma sub basin is a river basin located in the southwestern Tanzania. Katuma sub basin is part of the lake Rukwa river basin. A range of landforms including highlands, lowlands and plains characterizes the sub basin. It is also home to a variety of vegetation types including miombo and grasslands. The climate in the Katuma sub basin is characterized by a bimodal rainfall patterns with two rainy seasons the long rains are from March to May and the short rains from October to December. Due to its richness in vegetation cover it makes the Katuma sub basin to be an ideal for the study of analyzing the impact of climate variability on vegetation cover using the earth observation data.

The location map of the Katuma Sub Basin is shown in Figure 1.1, depicting the geographical extent and boundaries of the sub basin within the larger region.

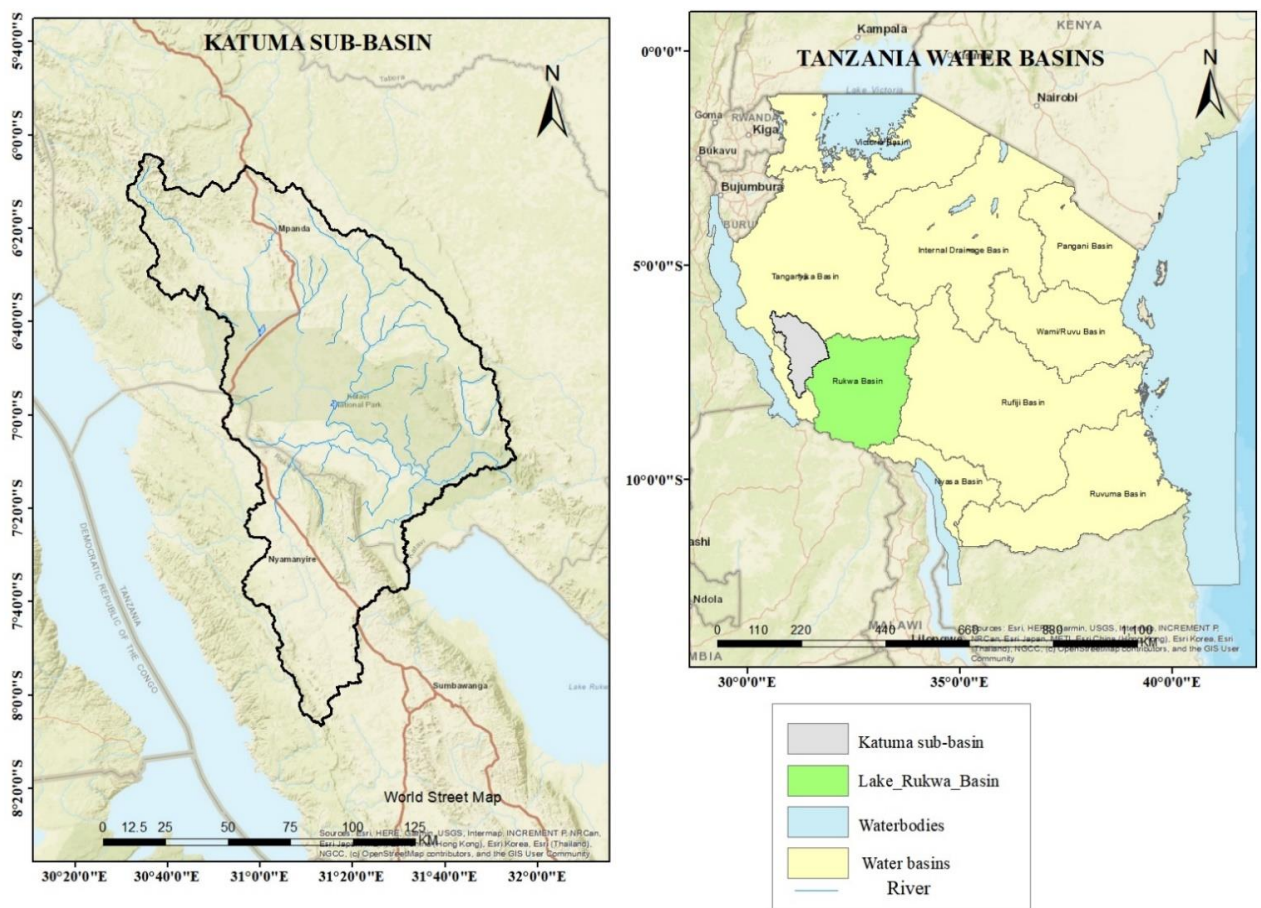


**Figure 1.1:** Location of the study area

## 1.8 Dissertation structure

This dissertation report has five chapters that are systematically organized in order achieve the intended goal of the study. Whereas;



## **Chapter one**

This chapter gives an overview of what the research is about and the general concept about the subject matter.

## **Chapter two**

It provides a detailed discussion on what other scholars have said concerning the issue researched as well as the related concepts. The major aim is to have a detailed understanding about the subject matter in relation to what is already known from other scholars.

## **Chapter three**

This chapter gives an illustration concerning the instrumentation, techniques and the systematic procedures followed in achieving the main goal of the research. All the methodological procedures from the acquisition of the data, data processing, data analysis and finally presentation of the obtained outputs are well explained in this chapter using the schematic diagram.

## **Chapter four**

Chapter four presents the research outputs as well as providing a detailed discussion on these outputs. It entails all the results obtained in accordance with their specific objectives and the overall results based on the main objectives as well as discussing them in details.

## **Chapter five**

This finalizes the whole study with the conclusion and recommendations concerning the research. The conclusion summarizes the findings that respond to the research questions and recommendation tells what next after this research has been done.

## **CHAPTER TWO**

### **LITERATURE REVIEW**

#### **2.1 Overview**

This chapter gives an overview of the concepts and definitions, which have been involved as well as the reviews of other scholars who have contributed to the accomplishment of this study. It has mainly covered the concept of remote sensing and its application in the extraction of features, Normalized Vegetation Difference Vegetation Index, correlation analysis and trend analysis. Literature review plays the most important part in the research as to which it enables us to acquire an understanding that has done and how other researchers have done it. Generally, it is an essential setting of focus of study and techniques to use when carrying out the research.

#### **2.2 Remote sensing in relation to vegetation cover and climate**

Remote sensing is the practice of deriving information about the earth's land and water surface using images acquired from an overhead perspective using the electromagnetic radiation in one or more regions of the electromagnetic spectrum, reflected or emitted from the earth surface (Campbell & Wynne, 2011b). Remote sensing uses the sensing devices that can either be passive or active sensors to record information about the object by measuring objects transmissions of electromagnetic energy from reflecting and radiating surfaces (Avtar et al., 2020). There are five types of resolution when discussing satellite imagery in remote sensing: spatial, spectral, temporal, radiometric and geometric (Campbell & Wynne, 2011a).

Satellite imagery has used to analyze changes in vegetation cover, deforestation and the impact of climate variability on the ecosystem. The study conducted by (Detto et al., 2018) satellite imagery has been used in the analyzing of impact of El Nino southern Oscillation of the Amazon rain forest during the El Nino years.

Landsat images this is the oldest continuous earth observing satellite imaging program. Optical Landsat imagery collected at a 30m spatial resolution since the early of 1980's. Starting with Landsat 5 thermal infrared imagery collected at a coarser spatial resolution than the optical data. Landsat7, Landsat 8 and Landsat 9 satellites are currently in orbit("Satellite Imagery," 2023). Landsat 5 with the Thematic Mapper (TM) sensor having seven spectral bands. Landsat 7 with the Enhanced Thematic Mapper sensor (ETM) has eight spectral bands. Landsat 8 sensor is Operational Land Imager and the Thermal Infrared Sensor (OLI/TIRS).

The Moderate Resolution Imaging Spectra radiometer (MODIS) this is the key instrument for the study of the earth's environment. MODIS provides data on different variables such as land

cover, vegetation cover and climatic variables. The MODIS sensor mounted on two satellites Terra and Aqua. The MODIS instrument has a spatial resolution of 250 meters and temporal resolution of two days (Vermote et al., 2015)

MODIS MOD09A1 is widely used dataset derived from the Moderate Resolution Imaging spectrometer (MODIS) sensor, which provides a wealth information on the land cover and vegetation characteristics at a global scale. MODIS MOD09A1 have been widely used in different fields including land cover and land change detection, forest biomass and ecological modelling. From (Wu et al., 2022) used the MODIS MOD09A1 data to map the spatial and temporal distribution of vegetation cover in the Tibetan plateau and found that MODIS MOD09A1 is an essential sensor for proving reliable information on the vegetation dynamics in the region. In addition, MODIS MOD09A1 used to monitor the impacts of climate on vegetation. The MODIS MOD09A1 data developed a model to predict climate change on the vegetation productivity in the Tibetan Plateau and found that it provides importance information for predicting the response of vegetation to the climate change (Wan et al., 2004). MODIS MOD09A1 is a valuable dataset that provides important information on land cover and vegetation characteristics globally. Despite its limitations such as the cloud, cover effect and atmospheric interference. MOD13Q1 dataset is a product derived from MODIS sensor aboard the terra and aqua satellite. This product provide the time series data on NDVI and Enhanced Vegetation Index (EVI). MOD13Q1 has a spatial resolution of 250 meters and the temporal resolution of 16 days. The spatial resolution makes it suitable for analyzing changes in the vegetation cover and productivity over large areas and monitoring the impact of climate variability on forest resources.

In this study remote sensing applicability, relies on the use of two satellites Landsat and MODIS as to which the Landsat satellite are essential in the determining the vegetation cover and the vegetation cover changes. The MODIS satellite using the MOD09A1 sensor is essential in determine of the Normalized Differenced Vegetation Index (NDVI) together with MOD13Q1 for obtaining the time series data of the NDVI.

The study of (Agrawala et al., 2003) to analyze the changes in climate variables, including temperature and rainfall, and their implications for the vegetation cover. They utilized remote sensing data to assess the vegetation dynamics and identify the trends associated with climate variability. However, their study primarily focused on a broader regional scale and did not specifically investigate the impact of climate variability on vegetation cover. Also, (Cloern et

al., 2016) emphasized the significance of remote sensing in understanding climate variability and its impact on ecological systems. They highlighted the ability of remote sensing to provide continuous and spatially explicit data on climate parameters and vegetation indices, enabling the detection of long-term trends and patterns. However, their study did not specifically address the impact of climate variability on vegetation cover.

### 2.3 Spectral indices on vegetation

Spectral indices are widely used in remote sensing to analyze changes in vegetation cover, land use and land cover changes. The Normalized Differenced Vegetation Index (NDVI) is one of the most widely used spectral indices for analyzing vegetation cover. The Normalized Differenced Vegetation Index (NDVI) developed by (Rouse et al., 1974) to estimate the amount of biomass. It takes into account the RED and Near Infrared bands (NIR). For the Landsat 5 and 7 it is the band 4 (NIR) and band three (RED). For the Landsat 8 and 9 it is band 5 (NIR) and band four (RED) respectively. To obtain NDVI is obtained from the ratio of the difference and summation of the near infrared band and the red band respectively as shown in the formula below.

$$NDVI = \frac{NIR-RED}{NIR+RED} \dots\dots\dots (2.1)$$

The NDVI is widely used to analyze changes in the vegetation cover; land use and land cover changes. The study conducted shows NDVI used to analyze the impact of climate variability on vegetation cover in Africa. The study found that there was a high correlation between NDVI and rainfall.

In the context of the Katuma sub-basin, the NDVI can serve as a valuable tool for assessing the impact of climate variability on forest cover. By calculating NDVI values using the appropriate spectral bands from Landsat satellite imagery, researchers can quantitatively analyze changes in forest vegetation over time. The relationship between NDVI and climate variables, such as rainfall, can provide insights into the effects of climate variability on the forest ecosystem. pattern.

### 2.4 Climate variability

Climate variability is an important factor affecting the vegetation cover in different regions. The climate in the Katuma sub basin characterized by two rainy seasons. However, in the last few decades there has been changes in the timing and intensity in the region resulting to climate variability (Zhang et al., 2019). The decline in the vegetation cover attributed to several factors including changes in the rainfall patterns, increased temperature and other anthropogenic

activities such as charcoal production and logging. The decline in the forest cover has led to several negative impacts including soil erosion, loss of biodiversity and reduced water availability. The loss of vegetation cover also affects the livelihood of the local communities who depend on forest for activities such as timber and other forest product.

The climate researcher shows that the decadal and multi decadal variability in rainfall that historically characterizes the country's climate is more likely to dominate the future changes in Tanzania (Campbell & Wynne, 2011). Thus, due to the uncertainty present of rainfall and temperature changes the overall impact of climate variability on vegetation though the variability present on climatic parameters.

## **2.5 Raster trend analysis**

Trend analysis is a robust to inter annual variability and is very effective procedure for focusing on the general nature of longer-term trends.(Liang et al., 2020). Trends may be linear slope of line fit to the time series such as the simple linear regression. The most commonly used to estimate the linear trend and the statistical significance

Student-t-test. The null hypothesis is no trend (an unchanging climate). The non-parametric trend mann-kendall test can also use to access monotonic trends both the linear or nonlinear significance. The mann-kendall test is much more sensitive to outliers and skewed distribution. The mann-kendall test often combined with Theil-Sen in the estimation of the linear trend. Things kept in consideration while analyzing trends include; the long-term observation estimate subjected to different sampling networks, the climate system within which the observation are made is not stationary, station, and ship and satellite are subjected to assort errors. Errors maybe random, systematic and external

The Mann-Kendall statistical test (Mann, 1945) has been widely used for detecting trends in the hydro metrological time series such as groundwater, stream flow, lake level, temperature and precipitation. The data used in the Mann-Kendall test should be independent (Wang et al., 2020)

## **2.6 Correlation analysis**

Correlation this is a bivariate analysis that measures the strength of the association between two variables and the direction of the relationship. The correlation coefficient varies from +1 to -1. +1 indicating strong correlation and -1 indicating weak correlation. The types of correlation are the positive correlation, negative correlation and zero or no correlation

In statistics, there are four methods correlation depending on the nature and purpose that are Pearson correlation, Kendall rank correlation, Spearman correlation and Point- Biserial correlation (Correlation (Pearson, Kendall, Spearman) - Statistics Solutions, 2023)

Pearson (r) coefficient is the widely used correlation statistic to measure the degree of relationship between linearly related variables. Assumption made in the Pearson coefficient is both variables should be normally distributed and linearity and homoscedasticity (data is equally distributed about the regression line). The Point-Biserial correlation conducted under the Pearson correlation formula except that one variable is dichotomous.

The correlation coefficient between variables x and y, denoted as  $r_{xy}$ , is a statistical measure that quantifies the strength and direction of the linear relationship between the two variables. It is calculated using the following formula

$$r_{xy} = \frac{n \sum x_i y_i - \sum x_i \sum y_i}{\sqrt{n \sum x_i^2 - (\sum x_i)^2} \sqrt{n \sum y_i^2 - (\sum y_i)^2}} \dots\dots\dots (2.2)$$

$r_{xy}$ =Pearson correlation coefficient between x and y

n=number of observation

$x_i$  =value of x for  $i^{th}$  observation

$y_i$ = value of y for  $i^{th}$  observation

Kendall rank correlation this is a non-parametric test that measures the strength of dependence between two variables.

The Kendall rank correlation coefficient, denoted as  $\tau$  (tau), is a non-parametric statistical measure used to assess the degree of association between two variables by comparing their rankings. It quantifies the similarity in the order of rankings between two sets of observations. The formula to compute Kendall's  $\tau$  is given by

$$\tau = \frac{nc - nd}{0.5n(n-1)} \dots\dots\dots (2.3)$$

$nc$  =number of concordant (ordered in the same way)

$nd$  =number of discordant (ordered differently)

Spearman rank correlation is a non- parametric test that used to measure the degree of association between two variables. It has no any assumptions about data distribution and is an appropriate correlation analysis when the data is measured in scale

The Spearman rank correlation coefficient, denoted as  $\rho$  (rho), is a non-parametric measure used to assess the strength and direction of the monotonic relationship between two variables. It is a valuable tool when dealing with ordinal or ranked data, where the exact numerical values may not be important, but the relative rankings are meaningful. The formula to compute Spearman's  $\rho$  is given by;

$$\rho = 1 - \frac{6 \sum d_i^2}{n(n^2 - 1)} \dots \dots \dots (2.4)$$

$d_i$  = the difference between the ranks of corresponding variables and  $n$  = number of observation  
(Correlation (Pearson, Kendall, Spearman) - Statistics Solutions, 2023)

## 2.7 Land Cover Mapping

Land cover mapping plays a crucial role in monitoring terrestrial ecosystems and climate modelling (Fischer & Getis, 2010). Satellite remote sensing is an essential tool for this purpose as it provides large-scale coverage and consistent data acquisition. Image classification is the process of assigning land cover classes to image pixels and falls under the category of pattern recognition. Machine learning algorithms used to develop models that can accurately classify land cover.

### 2.7.1 Image classification

Image classification falls in the category of pattern recognition, and it is tackled by developing appropriate machine learning algorithms. Machine learning algorithm used to train the computer on trying to produce the desired output from a set of inputs (Canty, 2014). The types of image classification that are the supervised and the un supervised classification.

#### i. *Supervised classification*

Supervised classification employed when the objects classified can be identified on the image. This method uses ground truthing data to classify images. It is a useful due to its ability to access the classification accuracy of the final product that is the land cover map (Konecny, 2014). The unknown pixels to one of the possible classes obtained from the training samples

#### ii. *Unsupervised classification*

This method is used when one cannot recognize the features present on the image. It involves the identification of the cluster on the image using iterative procedures. The obtained clusters can be checked using divergence to decide whether some clusters should be merged (Konecny, 2014). This type of classification used when the analyst is not familiar with the area of interest.

### 2.7.2 Classification schemes

These schemes provides taxonomically correct definitions of classes of information that organized according to logical criteria of the land cover and the land use classes. These schemes meant to guide the analyst in translating spectral classes into information classes. There are number of different classification schemes that have developed that incorporate both land cover and land use classes. One of such schemes is the American Planning Association Land- Based Classification Standards (LBCS). This scheme assists in extracting detailed urban and sub urban land use information from high spatial resolution remote sensing data. It often requires the use of in situ data or data obtained from aerial photographs (google earth).

Table 2.1 presents different land use and cover categories and their corresponding subcategories at various levels. This classification system can be helpful for studying and analyzing the distribution and characteristics of land use in a specific area or region.

Table 2.1: A summary of LULC classes as per Land-Based Classification Standard (Jensen, 2015)

<b>Level I</b>	<b>Level II</b>	<b>Level III</b>	<b>Level IV</b>
Urban or Built-up Land	Residential	Commercial and Services	Industrial
Agricultural Land	Cropland and Pasture	Orchards, Groves, Vineyards, Nurseries ,and Ornamental Horticultural Areas	Confined Feeding Operations
Rangeland	Herbaceous Rangeland	Shrub–Brush land Rangeland	Mixed Rangeland
Forest Land	Deciduous Forest Land	Evergreen Forest Land	Mixed Forest Land
Water	Stream and Canals	Lakes	Reservoirs
Wet Land	Forested wetland	Non-forested wetland	
Barren Land	Dry salt flats	Beaches	Sandy areas other than beaches
Tundra	Shrub and Bush Tundra	Herbaceous Tundra	Bare Ground Tundra

The classification of land use and cover types based on the four levels of Land-Based Classification Standards (LBCS) proposed by Jensen in 2015 is presented in Table 2.2. The table provides information on the typical data characteristics associated with each level, including the types of satellite imagery and aerial photography used at different spatial resolutions.



Table 2.2: Four levels of LBCS (Jensen, 2015)

Classification Level	Typical Data Characteristics
I	Satellite imagery such as NOAA AVHRR ( $1.1 \times 1.1$ km), MOD IS ( $250 \times 250$ m; $500 \times 500$ m), Landsat MSS ( $79 \times 79$ m), Landsat TM and Landsat 8 ( $30 \times 30$ m), and SPOT XS ( $20 \times 20$ m).
II	Satellite imagery such as SPOT HRV multispectral ( $10 \times 10$ m) and Indian IRS 1-C panchromatic ( $5 \times 5$ m). High-altitude aerial photography acquired at scales smaller than 1:80,000.
III	Satellite imagery with $1 \times 1$ m to $2.5 \times 2.5$ m nominal spatial resolution such as IKONOS. Medium -altitude aerial photography at scales from 1:20,000 to 1:80,000.
IV	Satellite imagery with $< 1 \times 1$ m nominal spatial resolution (e.g., GeoEye-1; Worldview -2). Low -altitude aerial photography at scales from 1:4,000 to 1:20,000 scale.

### 2.7.3 Separability analysis

The two statistical measures used to quantify the separability between different classes are parametric and the non-parametric statistical measures. The parametric separability analysis provides the covariance weighted distance between classes the values between 0 (no separable) and 2 (completely separable) (Jensen, 1996) To determine whether class signatures are separable as per the equation shown.

Equation (2.5) represents the relationship between transform divergence (TD) and divergence (D) as shown:

$$TD=2[1-\exp(-D8)] \dots\dots\dots (2.5)$$

Equation (2.6) calculates divergence (D) based on the values of C1, C2, C-11, C-12,  $\mu_1$ , and  $\mu_2$ . The equation involves various matrix operations and a trace function to obtain the final value of D

$$D = 12[(C1 - C2)(C - 11 - C - 12)] + 12tr[(C - 11 - C - 12)(\mu_1 - \mu_2)(\mu_1 - \mu_2)T] \dots\dots\dots (2.6)$$

Where  $TD$  is the transformed divergence between class 1 and class 2,  $C_1$  is the covariance matrix of class 1,  $\mu_{11}$  is the mean vector of class 1,  $tr$  is the matrix trace function, and  $T$  is the matrix transposition function. (Jensen, 1996)

#### 2.7.4 Classification algorithms

This algorithm uses the input training data to predict the likelihood that a certain class will fall into pre-determined categories. These algorithms are either from the supervised or unsupervised classification, and they typically use the classification logic to produce the classification map. The most commonly used classification algorithm is maximum likelihood and random forest.

Maximum likelihood algorithm assumes that the observed parameter for each class are normally distributed. Thus, it is the class that uses the variance-covariance matrix and that makes it most valuable. It calculates the probability of each pixel to belong to a pre-defined class and assigns the pixels to the class that has the highest probability (Jensen, 2015).

#### 2.7.5 Accuracy assessment

Accuracy assessment helps the user to assess the quantitatively how to fit the maps made from remote sensing imagery are fit for use. It shows the classification accuracy with confusion matrix also known as the error matrix. Such matrices shows the cross tabulation of the classified land cover and the actual land cover revealed by the sample site results. The confusion matrix has the values for the known land cover type in the column and the classified data in the rows. The main diagonal of the matrix lists the correctly classified pixels and those that are not in the main diagonal shows the divergence of each class from the correctly classified pixels. The accuracy assessment table has the user accuracy, producer accuracy, overall accuracy and the kappa coefficient (Xu et al., 2022)

##### i. *User accuracy*

User accuracy measures the reliability of the map. It shows how well the classified pixels represents what they say they represent. It is also referred to as the commission error; it is calculated by dividing the correctly classified pixels by the total number of pixels classified in that class (error of commission) as shown (Canty, 2014)

Equation (2.7) defines the user's accuracy (%) as the complement of the error of commission (%). It quantifies the correctness of positive predictions made by a classification or prediction model by subtracting the percentage of false positive results from 100%

$$\text{user's accuracy(\%)} = 100\% - \text{error of commission(\%)} \dots\dots\dots (2.7)$$

##### ii. *Producer accuracy*

Producer accuracy the measure of how well a certain area has been classified. It is also referred as the omission error. It is calculated by dividing the correctly classified pixels of a particular class with the summation of a whole column (error of omission) as show. The more errors of omission exist, the lower the producer's accuracy (Canty, 2014).

Equation (2.8) represents the producer's accuracy (%) as the complement of the error of omission (%). It measures the effectiveness of a classification or prediction model in correctly identifying the true positive cases by subtracting the percentage of false negative results from 100%

$$\text{producer's accuracy}(\%) = 100\% - \text{error of omission}(\%) \quad \dots\dots (2.8)$$

### iii. Overall accuracy

Overall accuracy answers the question of “what portion of the classification decision is correct?” The overall accuracy suggests the effectiveness of classification with no convincing evidence of the classification accuracy without evaluation of the full error matrix. It is calculated by dividing the sum of correctly classified pixels (diagonal) with total number of pixels examined (Campbell & Wynne, 2011)

Equation (2.9) defines the overall accuracy (%) as the ratio of the sum of diagonal elements (correctly classified pixels) to the total number of pixels examined in a classification or prediction process. It provides a comprehensive measure of the model's performance, indicating the percentage of correctly classified pixels among all the examined pixels.

$$\text{Overall Accuracy}(\%) = \frac{\sum \text{Diagonals}}{\sum \text{Pixels Examined}} \quad \dots\dots\dots (2.9)$$

### iv. Kappa Coefficient (k)

The kappa coefficient measures the overall agreement of a matrix. It also takes into account the non-diagonal pixels in the error matrix. It can be calculated as shown (Campbell & Wynne, 2011)

Equation (2.10) represents Cohen's kappa coefficient ( $\kappa$ ), a statistical measure used to assess the agreement between two raters or classifiers when dealing with categorical data. It is calculated by comparing the observed agreement ( $N \sum_{i=1}^r X_{ii}$ ) with the expected agreement due to chance ( $\sum_{i=1}^r X_{i+} X_{+i}$ ) and normalizing it by  $N^2$  times the sum of expected agreements.

Cohen's kappa coefficient is useful for evaluating the inter-rater reliability or the performance of a classifier in situations where chance agreements might influence the accuracy of the results

$$K = \frac{N \sum_{i=1}^r X_{ii} - \sum_{i=1}^r X_{i+} X_{+i}}{N^2 \sum_{i=1}^r X_{i+} X_{+i}} \dots\dots\dots (2.10)$$

Where:n

r = number of rows and columns in error matrix

N = total number of observations

$X_{ii}$  = observation in row i and column i

$X_{i+}$  = marginal total of row I, and

$X_{+i}$  = marginal total of column i.

## CHAPTER THREE

### METHODOLOGY

#### 3.1 Overview

The methodology part of this study divided into three parts whereas the part of vegetation cover extent this is from the NDVI and the land cover maps of different years. The second covers the determination of trend in the individual rainfall and temperature data and finally the correlation analysis part which seeks to determine whether the variation of the vegetation cover correlates the trends in climate change using the variables (temperature and rainfall). Workflow diagram (figure 3.1) to provide a visual representation of the data processing steps and analysis conducted during the study. It shows the sequential order of operations and how each step contributes to the results and conclusions

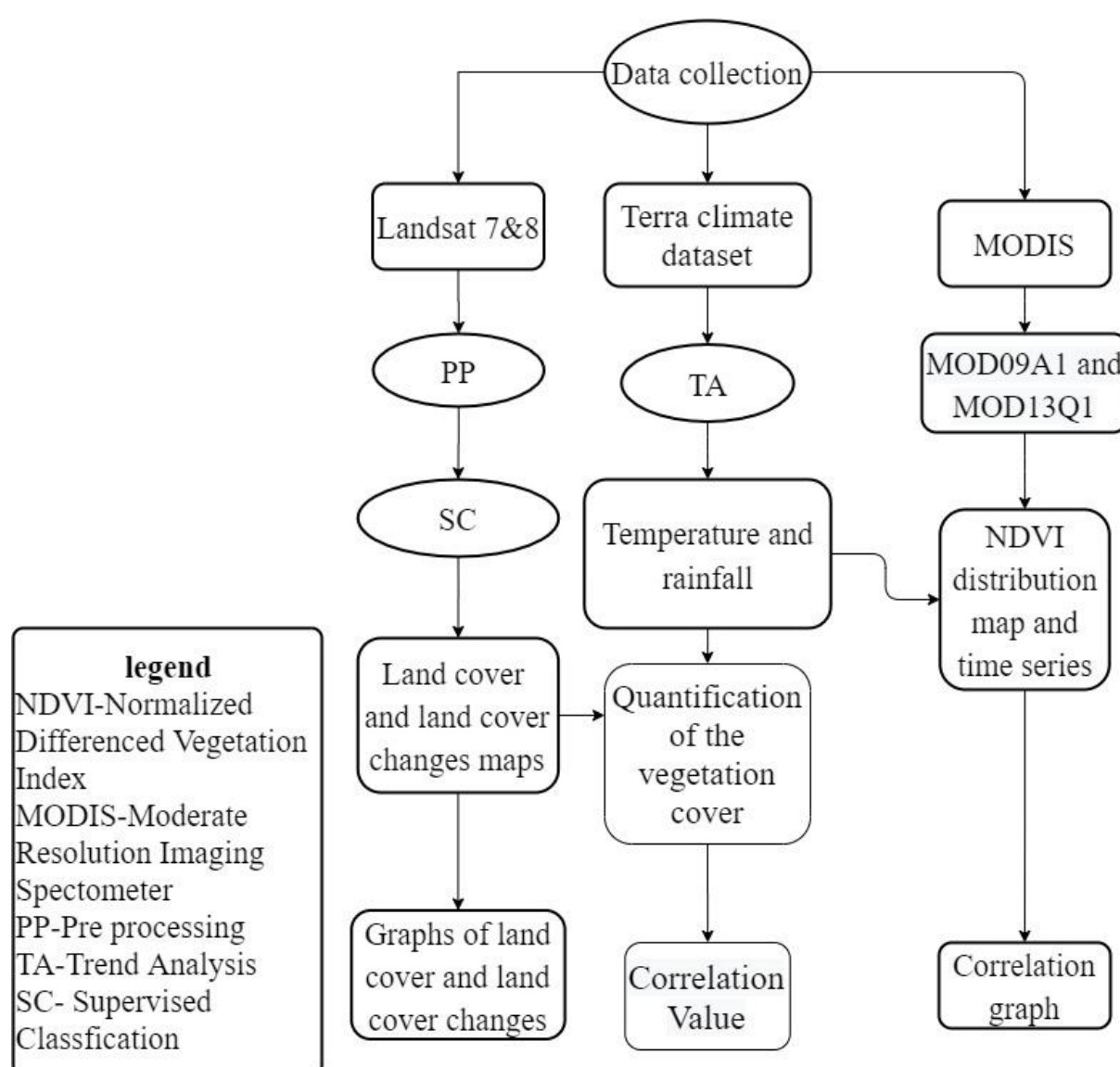


Figure 3.1: Methodology work flow diagram of the research

### 3.2 Data Acquisition

Data acquisition was the first step performed in which there were three kind of datasets required. That is the multispectral satellite imageries having spatial resolution of 30m in raster format, as well as the temperature and rainfall data from the terra platform having a spatial resolution of approximately 4km and MOD09A1 from the MODIS dataset with spatial resolution of 500m

#### 3.2.1 Landsat images

The satellite images data covering the study area downloaded from United States Geological Survey (USGS) through the link (<https://earthexplorer.usgs.gov>). The downloaded images were from Landsat 7 ETM and Landsat 8 OLI&TIRS from 2000 to 2020 ranging from January to October covering the Katuma sub basin with their spatial resolution of 30m. The cloud cover of these sub scenes were less than 10% and their respective path and row were (170, 65), (171, 64) and (171, 65). The three path and row covered the whole area of interest to ensure accuracy while studying the changes in the Katuma sub-basin forest cover. Table 3.1 shows the description of the Landsat image covering the study area.

Table 3.1 provides details about the Landsat data acquired for the study. The table includes information about the satellite, sensor, path/row, year, and the corresponding wavelength ranges for each band. Landsat 7 ETM+ and Landsat 8 OLI & TIRS images were obtained for the years 2000, 2010, and 2020, with various spectral bands used for analysis.

Table 3.1: Landsat data acquired

SATELLITE	SENSOR	PATH/ROW	YEAR
<b>Landsat 7</b>	ETM+	171/64	19/07/2000
		171/65	21/09/2000
		171/64	09/07/2010
		171/65	28/09/2010
<b>Landsat 8</b>	OLI & TIRS	171/64	24/07/2020
		171/65	18/09/2020

### 3.2.2 MODIS images

MODIS MOD09A1 producer is freely available from the NASA earth observations (NEO) website. The product is generated from the data acquired by the MODIS sensor onboard the Terra and Aqua satellites. The product is available in the HDF-EOS format and includes surface reflectance values at a 500-meter resolution. The downloaded images using band 1 and band 2 of the MOD09A1 that are the Near infrared and red band respectively they were used to calculate the NDVI of each year respectively. MOD13Q1 product are available in HDF-EOS format having the time series data of NDVI and the products are available for download from several data centers including NASA (National Aeronautics and Space Administration), EODIS (Earth Observation System Data and Information System) and USGS (United States Geological Survey). Table 3.2 showing the satellite, sensor, year, wavelength information for each band in MOD09A1.

Table 3.2 summarizes the attributes of the MODIS product, specifically MOD09A1. The table provides information about the bands, satellite, sensor, year, and corresponding wavelength ranges for each band. These attributes are essential for understanding the characteristics of the MODIS data used in the study.

Table 3.2: Table showing attributes of MOD09A1

band	satellite	Sensor	year	Wavelength(micrometer)
1	terra	MODIS	2000-present	0.620-0.670
2	terra	MODIS	2000-present	0.841-0.876
3	terra	MODIS	2000-present	0.459-0.479
4	terra	MODIS	2000-present	0.545-0.565
5	terra	MODIS	2000-present	1.230-1.250
6	terra	MODIS	2000-present	1.628-1.652
7	terra	MODIS	2000-present	2.105-2.155

### 3.2.3 TerraClimate Data

These were the data acquired from terra climate database using the link (<http://www.climatologylab.org/terraclimate.html>) with help of the Google earth Engine in the downloading of the data. Covering three climate variables that are temperature and rainfall in studying the climate changes. In addition, these data from the terra platform were in the interval of one year for each having an approximately spatial resolution of 4km (1/24°). The temperature in (°C), rainfall in (mm) covering a range of twenty years 2000-2020.

Table 3.3 presents a summary of the characteristics and sources of Terra climate data used in the study. The table outlines the spatial resolution, temporal resolution, and the temporal range for rainfall (mm), maximum temperature (°C), and minimum temperature (°C) data acquired from 2000 to 2020 at a resolution of 4km.

Table 3.3: Summary of Terra climate data characteristics and sources.

DATA	RESOLUTION		RANGE
	SPATIAL	TEMPORAL	
Rainfall (mm)	4km	Monthly	2000-2020
Maximum temperature (°C)	4km	Monthly	2000-2020
Minimum temperature (°C)	4km	Monthly	2000-2020

### 3.3 Software used

This includes the list of software used during the execution of the study. Table 3.3. Summarizes software for data preprocessing, processing, obtaining the expected outputs and finally analyzing the outputs.

Table 3.4: Software used in the study

SOFTWARE	VERSION	PURPOSE
ArcGIS	10.8	NDVI calculation, Image classification Mapping the classification outputs
R studio	3.6	For statistical analysis
Erdas imagine	2014	Image pre- processing
Draw.io	13.9.9	Preparing Research Schematic diagram
Google Earth Engine		Downloading climate data

### 3.4 Data preparation

At this stage, all datasets were prepared for processing purpose. It covers all the necessary steps in data preparation for both Landsat images and climate data as follows:

#### 3.4.1 Landsat images

This stage covers all the procedures required in obtaining necessary information from the images that is essential in processing part for obtaining the expected output. The preprocessing of the acquired Landsat images covered the following systematic procedures.



### **3.4.2 Layer stacking**

This refers to the process of combining more than one image bands with similar characteristics to form a single composite multi spectral image. Layer stacking performed as the first step of the preprocessing stage by importing the images from the .tif format to .tiff format. The Landsat images using the layer stacking tools of the Erdas imagine software 2014. Layer stacking performed to all images of Landsat 7 and 8.

### **3.4.3 Image re-projection**

The layer stacked Landsat scenes had the default image coordinate system used in the Landsat archive, which was projected coordinate system (UTM) to geographical coordinate system. World Geodetic System (WGS 1984). Applied to all images so that they referenced to a common coordinate system. The purpose of re projecting data from the UTM to geographic coordinate system was to avoid datum confusion since our study area falls in zone 36S.

### **3.4.4 Mosaicking**

All the scenes of each year mosaicked to form a single image that covers the entire study area. The study area was found on the (171, 65), (171, 64) scenes. This procedure applied in all the acquired images i.e. 2000, 2010 and 2020.

### **3.4.5 DE stripping**

This is the process of removing stripes or streaks from the images without disrupting the original image. Landsat 7 images had stripes during their acquisition using Erdas image software 2014 using the model maker tool the pixels having none digital number were assigned number using the model maker tool.

### **3.4.6 Image subset**

The mosaicked imaged were clipped to obtain the area of interest in order to reduce the processing time and storage for other processes. The clipping extent of the Katuma sub basin in a shape file extension.

### **3.4.7 Terra climate data**

The acquired terra climate data were prepared so as they can be processed in order to come up with the intended outputs showing how the climate has changed over the past twenty years of the study from 2000-2020. The climatic data included temperature both maximum and minimum annual temperature and annual mean rainfall. Using the R studio software version 4.3.0 the trends of these parameters obtained together with how they relate to each other and how do these parameters correlates with the NDVI.

### **3.4.8 MODIS data**

The data preparation in MODIS data (MOD09A1) involved converting the reflectance values to the top of atmosphere (TOA) reflectance this will account for the atmospheric effects. Then later use the Near Infrared Band and the Red band so as to calculate the NDVI value for each respective year and using the R studio to obtain the time series data for the NDVI.

## **3.5 Data processing**

This stage covers all the produces in the obtaining of the desired outputs. The aim is to produce output with respect to the research objectives as to which is analyzing the impacts of climate change on vegetation cover. The procedure for both vegetation cover and climate change as follows.

The satellite imagery aids in obtaining the land cover maps and in support with the appropriate software, it is able to obtain the land cover change maps, graphs and the quantified vegetation values. In the terra climate, data the data processing stage involved the use of R studio software in the plotting of the trends to all of the terra climate dataset. The MODIS (MOD09A1) data supports in the obtaining of the NDVI distribution map and the time series data of NDVI together with MOD13Q1 aid in obtaining time series data of NDVI

### **3.5.1 Normalized Differenced Vegetation Index (NDVI)**

This involves the calculation of the NDVI for all the images for delineating health of the vegetation present in Katuma sub basin. Its values ranges from -1 to 1 having four classes that are no vegetation, sparse vegetation, moderate vegetation and dense vegetation.

### **3.5.2 Regression analysis**

In this study, regression analysis used for determining the trend that exist in the temperature data (both minimum and maximum), and the rainfall data of the Katuma sub basin as the area of interest for studying the variability in the climate. The processing done in the R Studio software where the codes run in order to plot the data of the three respective climate variables. In this study, a linear regression model used to study the climate variability that have taken place within the region of interest. Through regression analysis, the trend of the temperature and rainfall for the twenty years studied was determined.

### **3.5.3 Classification**

The satellite Landsat imagery downloaded from the USGS were then classified using the supervised classification in ArcMap 10.4 software and analyzed the change detection of the vegetation cover. The following three main steps followed in carrying out classification.

- i. Training samples collected from the area of interest as per image. These samples randomly selected for each class. Whereas each class were contained in the area of interest that is water body, bare land, vegetation and built up areas
- ii. Performing parametric transform divergence separability analysis so as to determine if the classes are separable or not. Allowable separability is 1.5 to 2 (15,000 to 20,000) which indicates that the classes are separable.
- iii. Supervised classification of the study area was achieved using the maximum likelihood classifier, as since it is the classifier that used the variance-covariance matrices and its portable due to its simplicity and effectiveness in handling multi class classification problems. Maximum likelihood classifier considers pixels that have the highest probability to belong to a particular class and assigns it there.
- iv. Accuracy assessment performed to check the accuracy of the classified images. This achieved by using the higher resolution Google earth images from google earth pro respective year classified. The higher resolution image were used in the validation data to collect the sample points from the respective year used in the performing of the accuracy assessment.

Points were randomly selected from the area of interest of the classified image exported in the KML shape file so as they can viewed in the google earth pro software. After performing point validation confusion matrix using the ground truthing from the google earth pro used to match to those of the classified image to obtain the user accuracy, producer accuracy the overall accuracy together with the kappa statistic of all the years of the land cover images.

### **3.6 Data analysis**

This section presents how data analyzed in order to come up with the expected output to meet the main objective of the study. In this study, it covers the Mann Kendall test that aids in the detection of trends in the time series data, correlation analysis of the NDVI and the results obtained from the regression analysis data of precipitation and correlation between the quantified vegetation cover and the climatic parameters.

#### **3.6.1 Mann-Kendall test**

This is the statistical test used to analyze trends in time series data. It detects the monotonic trends in time series data, which means trends that either increase or decrease over time without reversals. Thus, used to analyze trends in climatic parameters (temperature and rainfall).

#### **3.6.2 Correlation analysis**

For obtaining the correlation between NDVI and the precipitation computation, and the correlation between quantified vegetation cover and climatic parameters done in R studio. With

the basis of Pearson correlation that developed by Karl Pearson shown in equation 3.3. The relationship between NDVI and precipitation computed. Direction of value of R which ranging from -1 to 1 if it is directly proportional related or inversely proportional to both two variables in order to show how the impact of the climate variability on vegetation cover in Katuma sub basin for the respective years from 2000-2020. Additionally the correlation between the quantified vegetation cover from the land cover with the climatic parameter obtained to show how these two data sets relate to each other. Moreover, show the relationship between them.

## CHAPTER FOUR

### RESULTS AND DISCUSSION

#### 4.1 Overview

This chapter presents the results of the research findings as well as the discussion of these results. It covers both the land cover and land cover changes, Normalized Differenced Vegetation Index (NDVI) and the climate change together with the results showing the correlation between the NDVI and the climate parameter together with correlation of quantified vegetation values and the climatic parameters.

#### 4.2 Normalized Differenced Vegetation Index (NDVI)

The analysis of the Normalized Difference Vegetation Index (NDVI) data for the Katuma sub basin from 2000 to 2020 reveals interesting insights into the vegetation health of the region. Figure 4.1 displays the NDVI distribution map, showing four vegetation classes with distinct ranges of NDVI values. Throughout the study period, there was generally a significant presence of healthy vegetation, except for a noticeable decline in vegetation health in 2007. This is evident from the lower NDVI values (0.7991) observed during that year. Figure 4.2 presents the NDVI time series plot, which depicts the annual distribution of NDVI values. It is noteworthy 2010 exhibited peak NDVI values, indicating a higher level of vegetation health during those years. On the other hand, 2007 recorded a sharp decrease in vegetation health with a very low NDVI value. Importantly, the statistical analysis confirms the significance of the NDVI time series. The calculated p-value, which measures the association between NDVI, found not to be statistically significant at the chosen significance level of 0.05. This implies that the trend of the vegetation health does not actually depicts the actual values. Furthermore, the regression equation obtained from the analysis reveals a positive slope, indicating a gradual increase in NDVI values over the study period. This suggests a nourishment in vegetation health within the Katuma sub basin. Overall, these findings provide valuable insights into the changes in vegetation health and highlight the importance of monitoring NDVI as an indicator of environmental dynamics.

Figure 4.1 displays the NDVI distribution map for the years 2000 to 2020. The table provides a comprehensive overview of the normalized difference vegetation index (NDVI) values across the study area for each respective year.

Figure 4.2 presents the NDVI time series data spanning the years 2000 to 2020. The table provides a chronological overview of the normalized difference vegetation index (NDVI) values over the specified period, highlighting the temporal trends in vegetation cover.

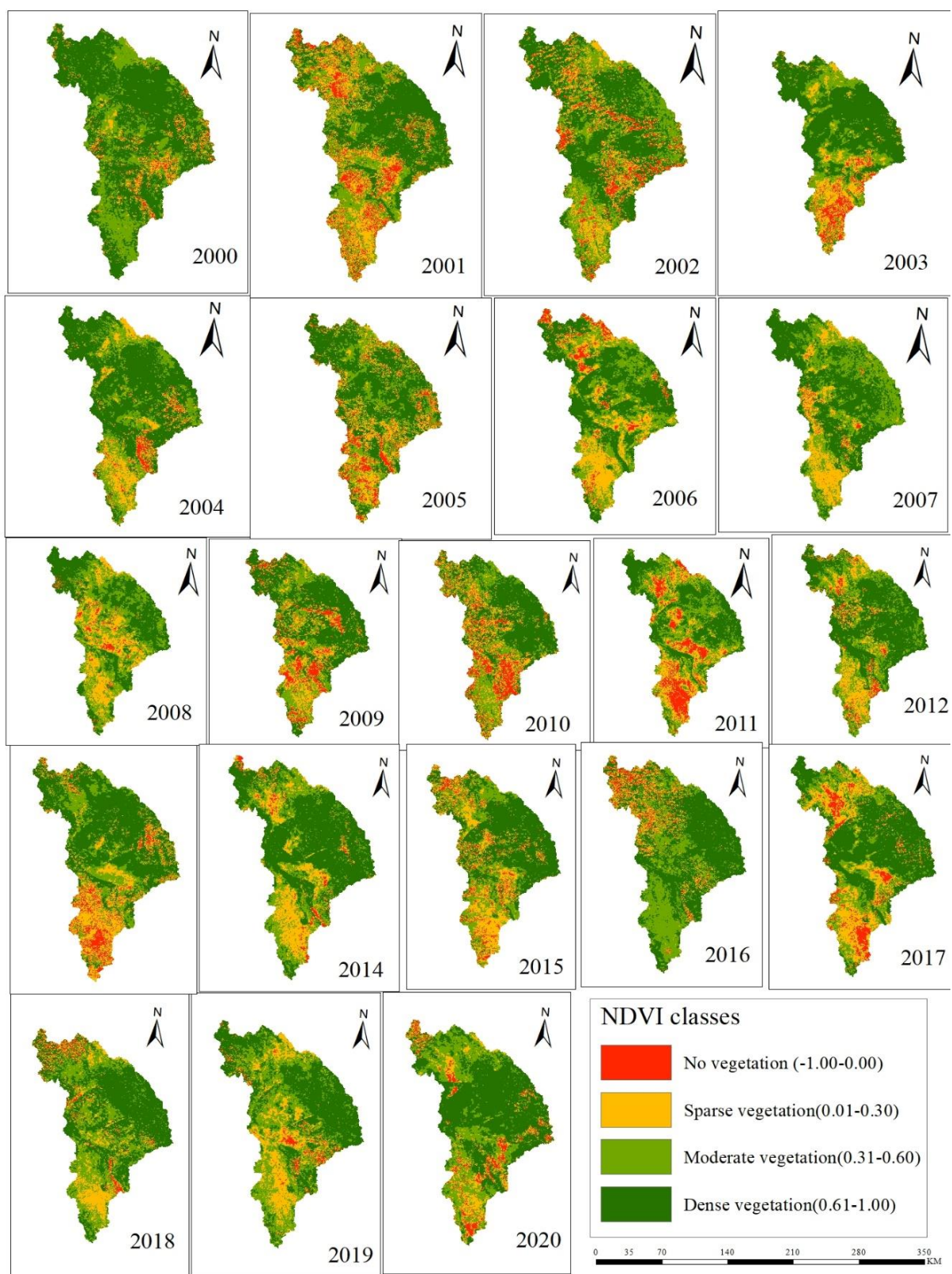


Figure 4.1: NDVI distribution map of Katuma Sub-Basin (2000-2020)

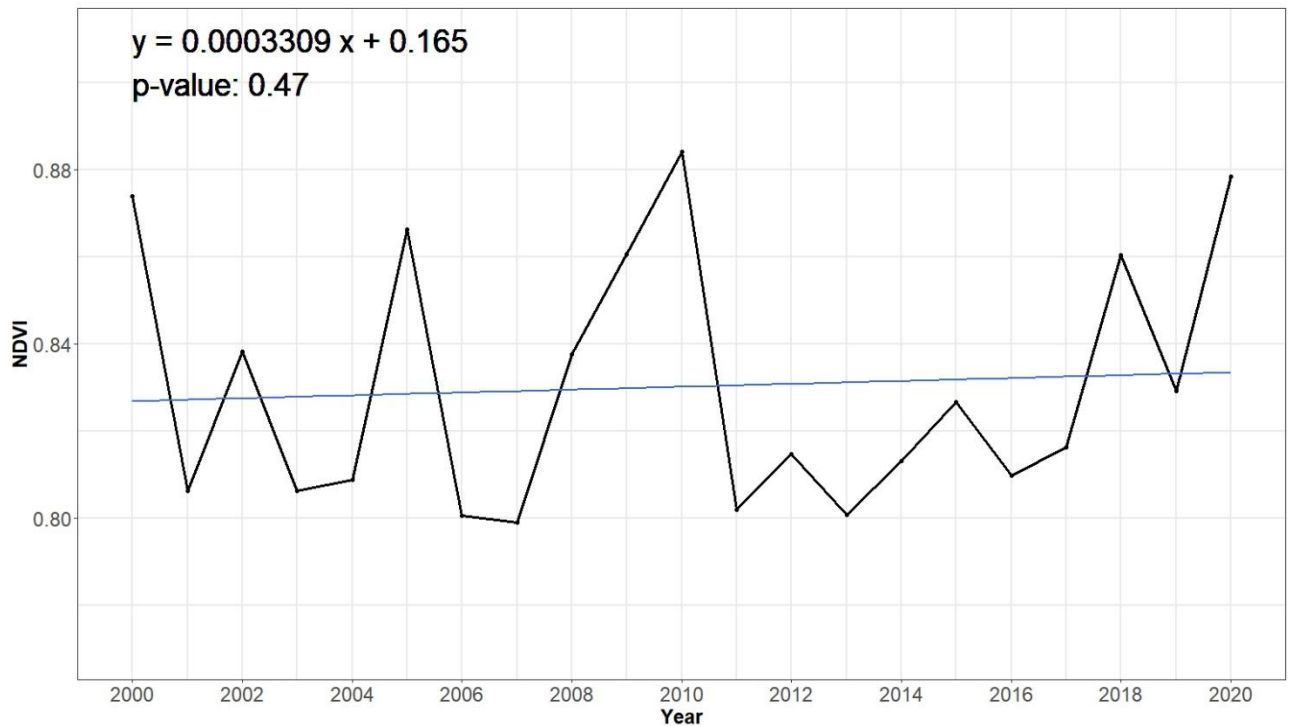


Figure 4.2: NDVI time series of Katuma Sub-Basin 2000-2020

### 4.3 Climate change

The climate change results based on two major climatic variables (rainfall and temperature) by considering how they been over the whole period studied. These are as follows.

#### 4.3.1 Annual Maximum Temperature trend

The variability in the maximum temperature shows the positive trend within the data. Figure 4.3 shows the slope of the linear regression line for the plotted maximum temperature data is 0.01109 this signifies that the overall increase in annual temperature with in the period of 2000-2020. The P value with a used significance level of (0.05) shows its value being less than that of the significance level that is 0.0201. Hence, it indicated that there is the null hypothesis accepted hence, it is statically significant.

Figure 4.3 displays the time series trend of maximum annual temperatures. The table provides a chronological representation of the maximum temperature values across the study period, allowing for an assessment of the temperature trend over the years.

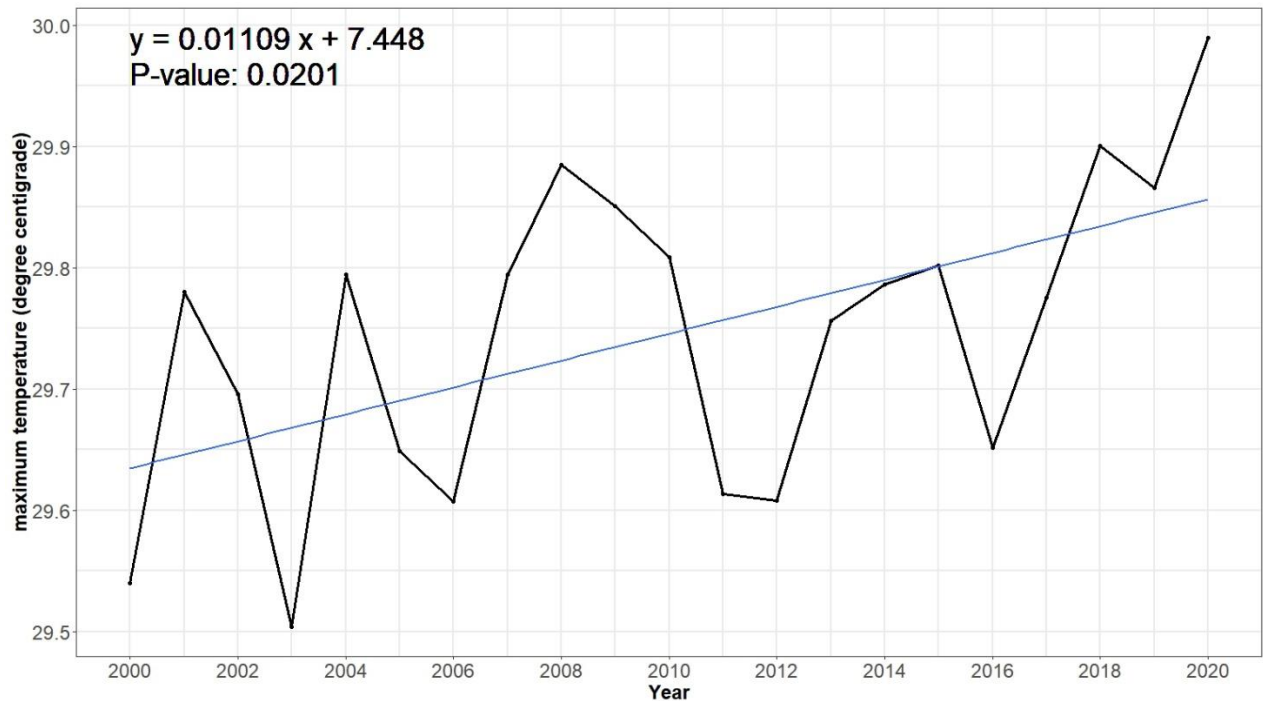


Figure 4.3: The annual maximum temperature trend of Katuma Sub-Basin 2000-2020

#### 4.3.2 Annual minimum temperature trend

Figure 4.4 shows a positive slope of 0.01323 in the regression equation, indicating an overall increase in annual minimum temperature over the study period. This suggests that the minimum temperature has been gradually rising from 2000 to 2020. The calculated p-value of 0.0497 suggests that the trend in annual minimum temperature of Katuma sub basin is statically significant. Since the p-value is less than the chosen significance level of 0.05, we can conclude that the observed relationship is unlikely to be due to random chance. Therefore, the relationship between the minimum temperature and year closely represents the true trend of the minimum temperature variation over time.

The analysis indicates a positive trend in the minimum temperature variability from 2000 to 2020. Furthermore, the statistically significant p-value supports the conclusion that the observed relationship is not a result of random chance. The regression equation provides a quantitative understanding of the relationship between the year and the minimum temperature annually.

Figure 4.4 highlights the trend in minimum annual temperatures over the study period. The table presents a chronological depiction of the minimum temperature values, enabling an analysis of how the minimum temperatures have changed from year to year.



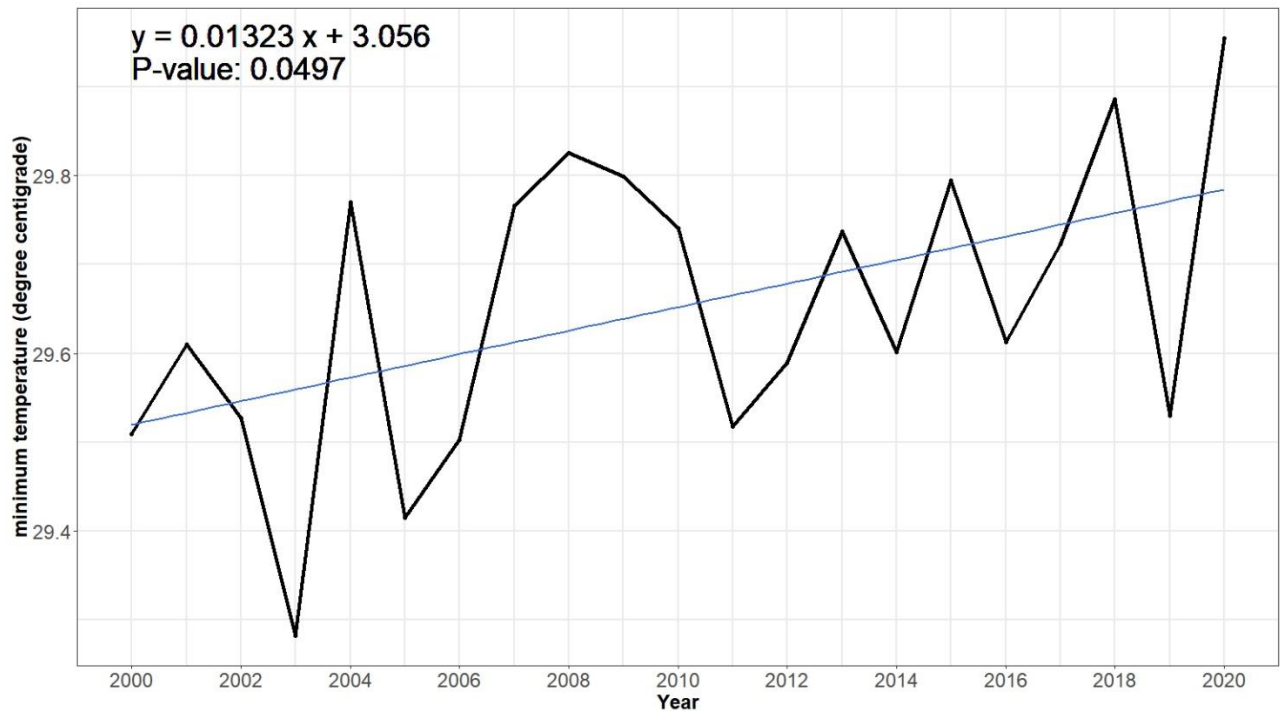


Figure 4.4: The annual minimum temperature trend of the Katuma Sub-Basin 2000-2020

#### 4.3.3 Overall temperature trend

As depicted in Figure 4.5. This indicates that there has been a consistent rise in temperature over the twenty-year period. The observed temperature trend aligns with broader global climate change patterns, where increasing temperatures are a key indicator of climate change. The warming trend observed in the Katuma sub basin is likely influenced by both local and global factors, including greenhouse gas emissions, land-use changes, and natural climate variability. The analysis indicates a clear and consistent increase in maximum and minimum temperatures over the 2000-2020 period. This upward temperature trend contributes to climate variability within the forest cover of the Katuma sub basin, with potential ecological and socio-economic consequences. Continued monitoring and analysis of temperature trends will be essential for assessing the long-term impacts and developing appropriate measures to mitigate and adapt to the changing climate conditions in the region.

Figure 4.5 presents the overall temperature trend observed throughout the study period. The figure provides a graphical representation of the temperature variations over the years, offering insights into the general temperature patterns

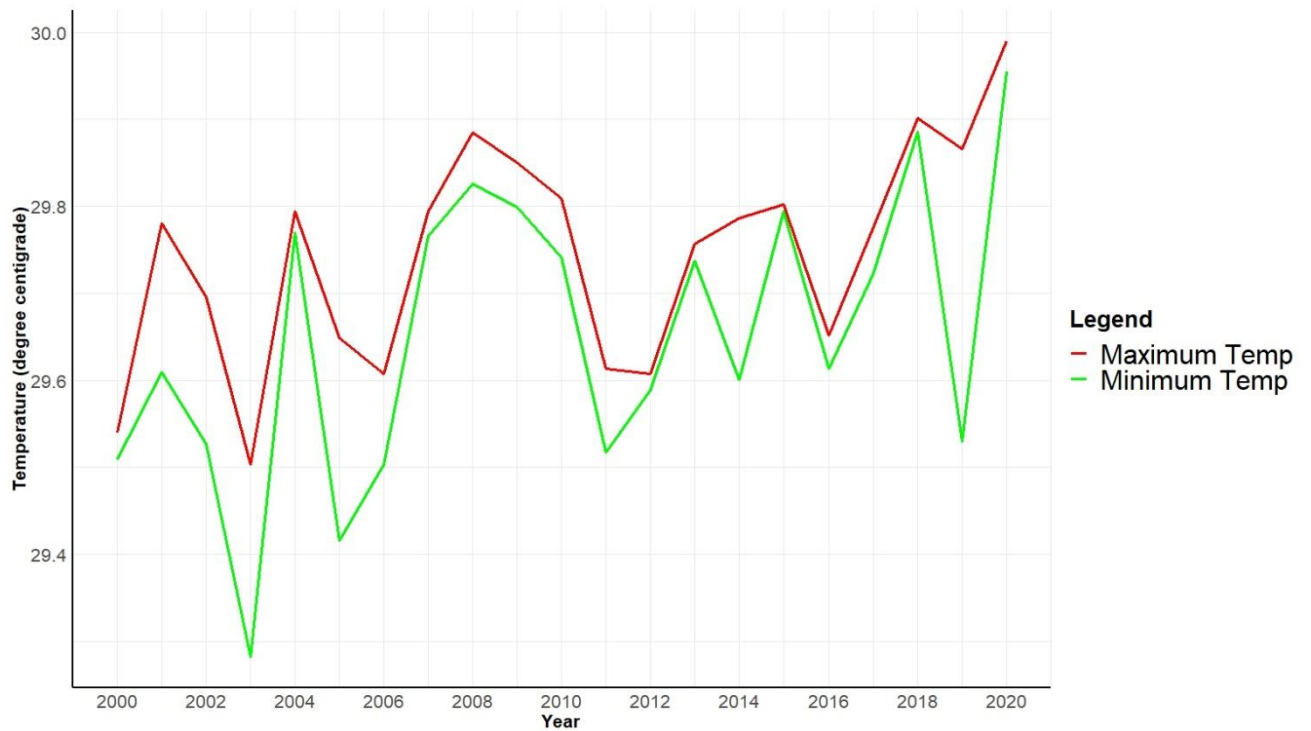


Figure 4.5: The overall maximum and minimum temperature trend of Katuma Sub-Basin 2000-2020

#### 4.3.4 Annual rainfall trend

The annual rainfall shows a positive trend in the variability within the processed terra-climate rainfall data. This implies that the annual has been increasing from the year 2000-2020. Hence, contribution a lot to the overall climate variability with in the region since, it one among the major climate variables involved in the climate change analysis. From the regression equation, it shows the slope of 4.8. The positive sign signifies that the trend of rainfall over time is increasing over the period of twenty years 2000-2020. The P value of 0.0275 under the significance level of 0.05 signifies that there is statically evidence to reject the null hypothesis of no trend in the data at the significance level of 0.05 since the P value is lower than the 0.05 significance level. Hence, the trend strongly depicts the actual trend present in the Katuma sub basin. The increasing trend in annual rainfall has significant implications for water resources, agriculture, and the overall climate change scenario in the region. It highlights the need for adaptive measures and sustainable water management strategies to cope with the changing rainfall patterns and ensure the resilience of ecosystems and communities in the Katuma sub basin. The statistically significant p-value reinforces the validity of the observed trend. It is crucial to closely monitor and assess rainfall patterns to inform climate change adaptation and water-resource management strategies in the Katuma sub basin.

Figure 4.5 presents the overall temperature trend observed throughout the study period. The figure provides a graphical representation of the temperature variations over the years, offering insights into the general temperature patterns

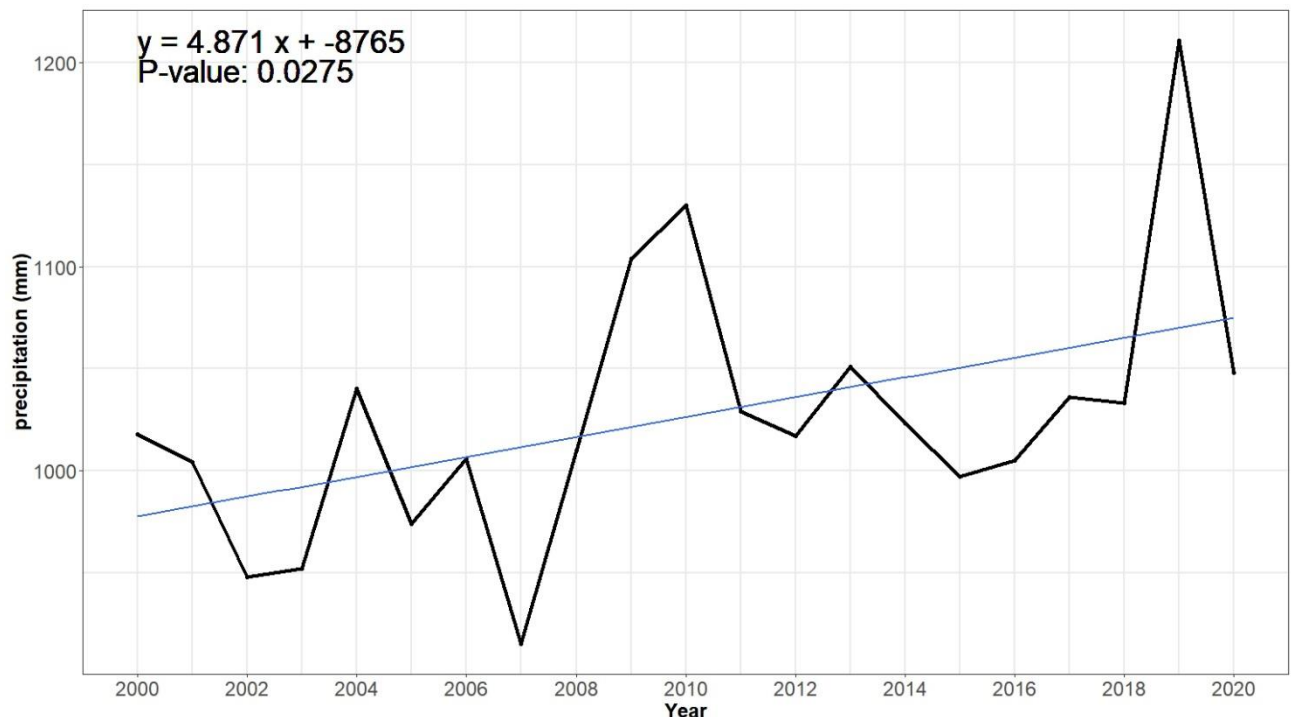


Figure 4.6: The annual rainfall trend of Katuma sub basin 2000-2020

#### 4.4 Mann Kendall results

The Mann Kendall result table showing the variables together with the climatic parameter displayed as shown on table 4.1. The chosen significance level for the test was 0.05 in which it aided in the determining the threshold for the statically significance.

The Kendall Tau in which it indicated as the S score measures the strength and direction of the rank between the variables. Thus, from our table the precipitation trend, the maximum and minimum temperature shows the increase in trend shown by the positive in the S score. Whereas the positive value shows increase.

The Z value represents the standard score indicating how standard deviation the observed Kendall Tau is from the expected value under the null hypothesis of no trend. If the Z value exceeds the critical value, corresponding to the chosen significance level it indicates a statically significance in trend. For maximum and minimum temperature and precipitation, the observed value is above the mean. Thus, statically the values are much higher than the expected value

The P value signifies the statically significance of the Mann Kendall results due to the over shoot and under shoot of the climatic data he Mann Kendall test is a preferable test to test the significance of the trend. For precipitation, maximum and minimum temperature they are all statically significant thus, they can depicts the true trend of the variables present since they are all below the chosen significance level of 0.05

The results of the Mann Kendall test provide valuable insights into the climatic patterns of the study area. The decreasing trend in precipitation indicates a potential decline in rainfall over time, which can have significant implications for water resources, agriculture, and ecosystems. Conversely, the increasing trends in maximum and minimum temperature suggest a warming climate, with potential impacts on various aspects of the environment and human activities.

Table 4.1 provides the results of the Mann-Kendall test conducted on climate data variables. The table presents information about the observed trend, S-score, variance of S, Z-score, and corresponding p-value for precipitation, maximum temperature, and minimum temperature. These results offer insights into the trends and statistical significance of the analyzed climate variables.

Table 4.1: Mann Kendall result

<b>climate data</b>	<b>Trend</b>	<b>S-score</b>	<b>var (S)</b>	<b>Z-score</b>	<b>P-value</b>
Precipitation	increasing	74	1095.67	2.0543	0.02749
maximum temperature	Increasing	116	1096.67	3.4742	0.00052
minimum temperature	Increasing	70	1096.67	2.0845	0.0372

#### 4.5 Correlation results

The correlation analysis was conducted to explore the relationship between NDVI and rainfall, specifically using the Pearson correlation coefficient. The calculated coefficient of 0.68 indicates a positive correlation between the two variables. This suggests that when rainfall increases, there is a corresponding increase in NDVI, indicating a positive relationship between vegetation health (as indicated by NDVI) and precipitation.

The P value of 0.00063, with a significance level of 0.05, suggests that we cannot reject the null hypothesis that there is a significant correlation between NDVI and rainfall. This means that the observed correlation could not be due to random chance rather than a true relationship between the variables.

Figure 4.7 depicts a correlation plot illustrating the relationship between the normalized difference vegetation index (NDVI) and precipitation. The figure visually represents the correlation between these two variables, providing insights into how changes in precipitation relate to variations in vegetation cover.

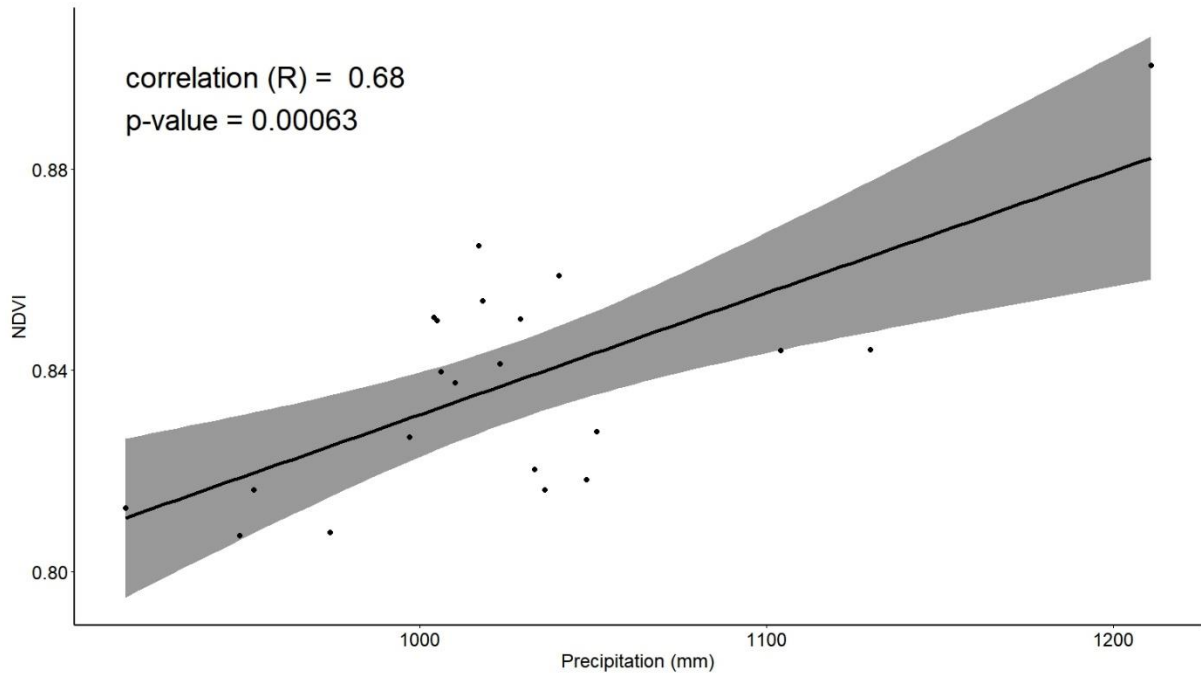


Figure 4.7: Correlation plot between NDVI and rainfall of Katuma sub basin 2000-2020

#### 4.6 land cover

With reference to the American Planning Association Land Based Classification Standards (LBCS) level 1, figure (4.8.4.9 and 4.10) shows the nature of forest cover at the Katuma sub basin for the years 2000, 2013 and 2020. These maps provide valuable insights into the distribution and changes in land cover classes, including built-up areas, bareland, vegetation, and water bodies. It can be observed that a significant portion of the sub basin was covered by vegetation, indicating a relatively healthy forest cover. There are limited built-up areas, suggesting minimal human settlement and infrastructure development at that time. The presence of water bodies indicates the existence of rivers, lakes, or other water features within the sub basin. The presence of bareland suggests areas with limited or no vegetation cover, which could be due to natural factors such as soil erosion or human activities such as agriculture or deforestation (Leweri et al., 2021).

Figures 4.8, 4.9 and 4.10 display the land cover maps of the Katuma sub basin for the years 2000, 2010, and 2020, respectively. These figures visually present the land cover classification

results for each respective year, offering insights into the changes in land cover over the specified period

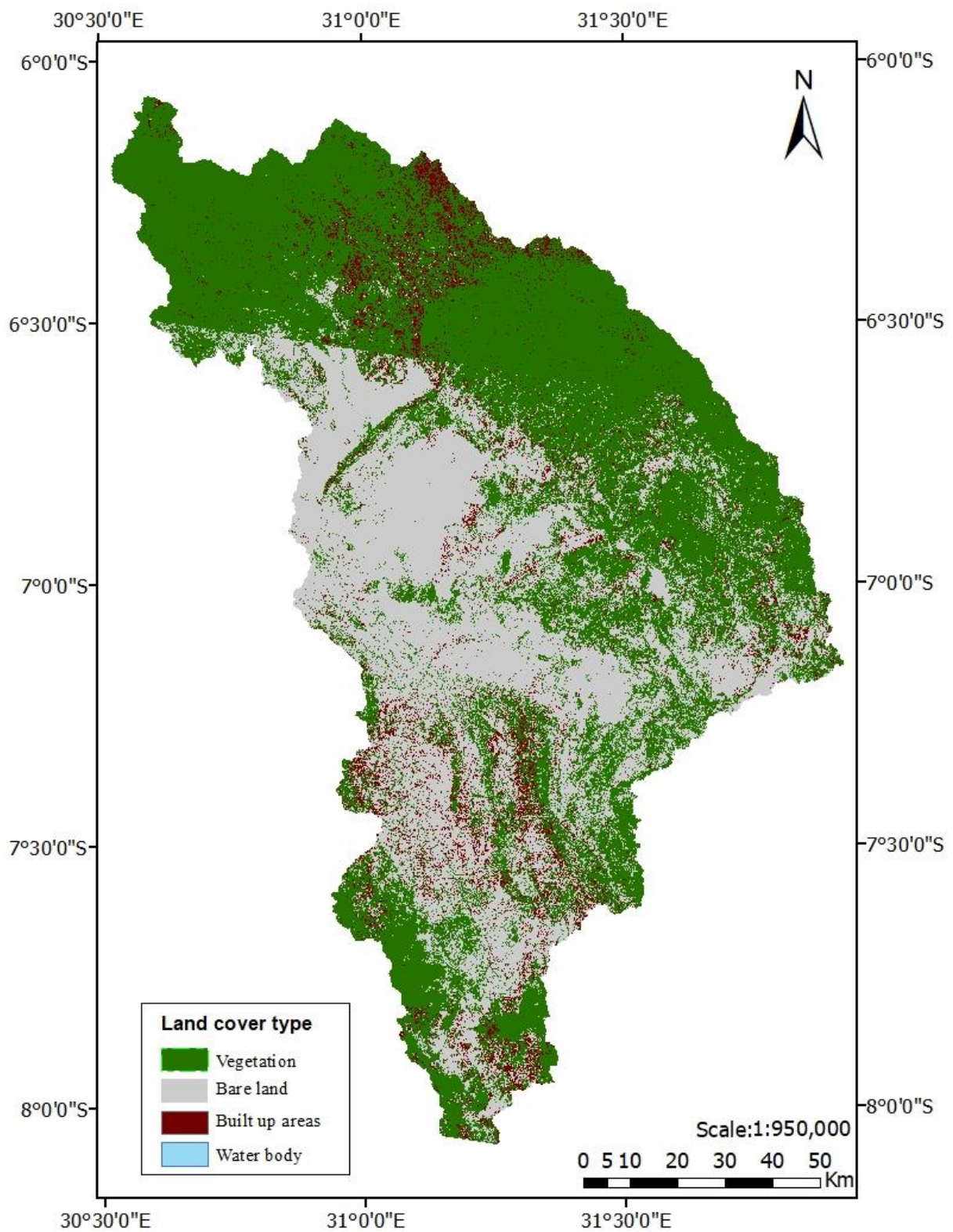


Figure 4.8: Land cover maps on vegetation cover in the Katuma Sub-Basin of 2000



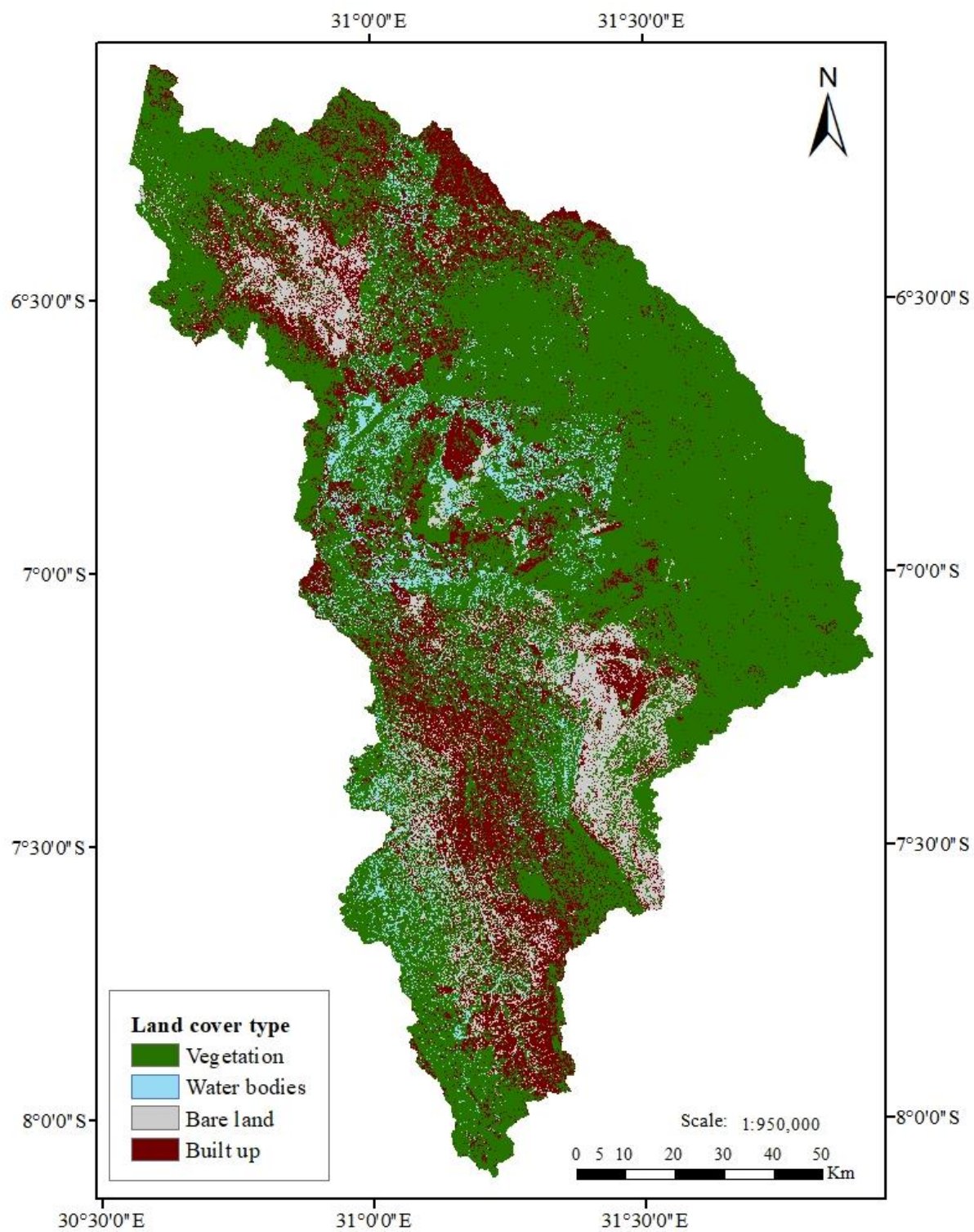


Figure 4.9: Land cover map on vegetation cover in Katuma Sub-Basin of 2010



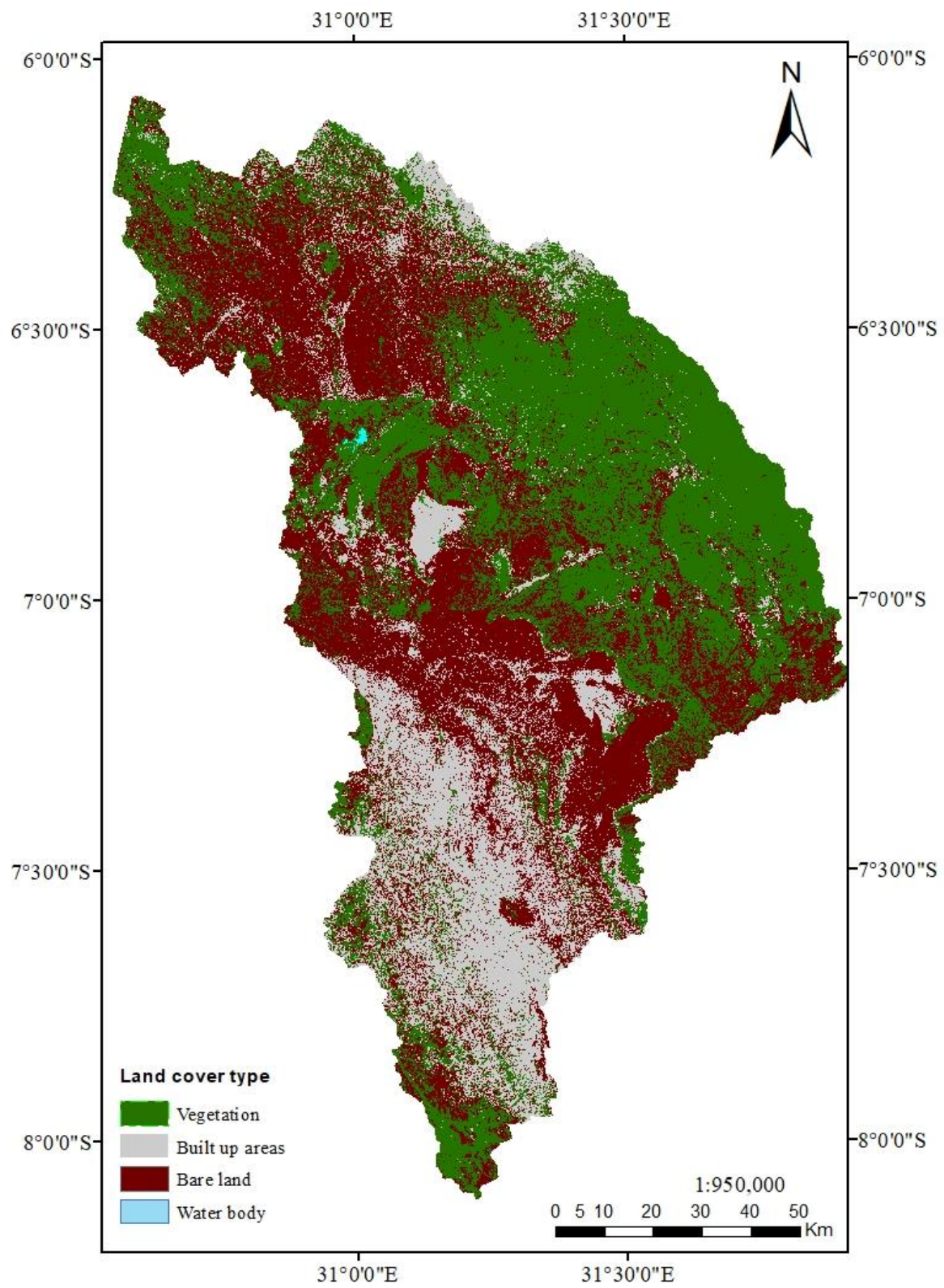


Figure 4.10: Land cover map on vegetation cover in Katuma Sub-Basin 2020

#### 4.6.1 Accuracy assessment

The accuracy assessment of the classified images for the year 2000, 2013 and 2020 are represented in table 4.2, 4.3 and 4.4 respectively. The accuracy assessment results indicate varying levels of accuracy and reliability for different land cover classes and across different years. The classification of Vegetation and Built-up areas generally shows higher accuracy, while the classification of Water bodies and bare land may have some limitations. It is important to consider these factors when analyzing and interpreting the land cover maps for the respective years.

Table 4.2 presents the confusion matrix for the classified image of 2000. The table includes class values, user accuracy, producer accuracy, and kappa statistics for various land cover classes such as vegetation, bare land, built-up areas, and water bodies.

Table 4.3 displays the confusion matrix of the classified image of 2010. The table provides information on user accuracy, producer accuracy, and kappa statistics for different land cover classes including vegetation, water bodies, bare land, and built-up areas.

Table 4.4 presents the confusion matrix of the classified image of 2020. The table includes user accuracy, producer accuracy, and kappa statistics for vegetation, built-up areas, bare land, and water bodies.

These tables offer insights into the accuracy and reliability of the land cover classification results for the respective years.

Table 4.2: Confusion matrix for the classified image of 2000

<b>Class value</b>	<b>Vegetation</b>	<b>Bare land</b>	<b>Built up areas</b>	<b>Water body</b>	<b>Total</b>	<b>User accuracy</b>	<b>Kappa</b>
Vegetation	40	4	5	0	52	0.77	0
Bare land	6	41	0	0	47	0.87	0
Built up areas	0	0	1	0	1	1	0
Water body	3	0	0	0	3	0	
Total	49	45	6	0	100	0	0
Producer accuracy	0.82	0.91	0.17	0	0	0.82	0
Kappa	0	0	0		0	0	0.66

Table 4.3: Confusion matrix of the classified image of 2010

<b>Class Value</b>	<b>Vegetation</b>	<b>Water bodies</b>	<b>Bare land</b>	<b>Built up areas</b>	<b>Total</b>	<b>User accuracy</b>	<b>Kappa</b>
Vegetation	53	0	7	2	62	0.85	0
Water bodies	4	0	0	0	4	0	0
Bare land	1	0	7	0	8	0.88	0
Built up areas	3	0	5	20	28	0.71	0
Total	61	0	19	22	102	0	0
Producer accuracy	0.87	0	0.37	0.91	0	0.80	0
Kappa	0	0	0	0	0	0	0.62

Table 4.4: Confusion matrix of the classified image of 2020

<b>Class Value</b>	<b>Vegetation</b>	<b>Built up areas</b>	<b>Bare land</b>	<b>Water bodies</b>	<b>Total</b>	<b>User accuracy</b>	<b>Kappa</b>
Vegetation	33	0	3	0	36	0.92	0
Built up areas	1	27	4	0	28	0.96	0
Bare land	11	2	35	0	48	0.73	0
Water bodies	4	0	0	4	8	0.5	0
Total	46	15	39	4	120	0	0
Producer accuracy	0.72	1.80	0.90	1	0	0.83	0
Kappa	0	0	0	0	0	0	0.76

#### 4.6.2 Separability analysis

The four classes (built up areas, vegetation, Bare land and water body) tested by the tran61sform divergence to see if they are separable or not. The classes were separable as since they ranged from 15,000-20,000 in which it is the acceptable separability. Table 4.2 shows the average value range for each year. Therefore, it can be concluded that the classes are separable in all three years, indicating that they can be distinguished from each other based on the

characteristics of the land cover. This information is valuable for further analysis and interpretation of the land cover maps, as it confirms that the classes are distinct.

Table 4.5 presents the separability values for different years. The table provides the average separability values calculated for the years 2000, 2010, and 2020, indicating the level of separability between different land cover classes in each respective year.

Table 4.5: Separability table

Year	Average separability value
2000	15,371
2010	15,102
2020	15,966

#### 4.6.3 Quantification of the land cover

There are significant changes in the land cover classes over the period of 2000-2020. This is due to some of the both natural and anthropogenic activities that undertaken in the Katuma sub basin. Water bodies showed a relatively small quantification value compared to other classes where as it seen that the construction activities in the Katuma sub basin increases. It is even widely shown from the map that areas of Mpanda show increase in the built up activities and bare land decreased over the period. Vegetation showed some fluctuations over time in which the degree of variability are influenced by factors such as climate variability, land management practices and some natural disturbances such as fire or drought.

The fluctuations in land covers observed over the studied years can be attributed to various factors and processes that influence the environment. These fluctuations are indicative of changes in the distribution and composition of different land cover classes within the Katuma sub basin. Several key factors can contribute to these fluctuations:

**Urbanization and Development:** The increase in built-up areas from 2000 to 2020, as shown in Table 4.6, suggests urbanization and development. Rapid population growth, industrialization, and infrastructure expansion can lead to the conversion of natural landscapes into built-up environments, altering the land cover composition.

**Land Use Changes:** Changes in land use practices, such as conversion of agricultural land to built-up areas or shifting cultivation practices, can influence land cover fluctuations. These changes can be driven by economic, social, and policy factors.

**Climate Variability:** Fluctuations in precipitation and temperature, as indicated by the Mann-Kendall results (Table 4.1), can impact vegetation and water body dynamics. Changes in climate conditions can affect vegetation health, leading to shifts in the extent of vegetation cover and water bodies.

**Natural Disturbances:** Natural events like wildfires, floods, and droughts can have immediate and long-term impacts on land cover. These disturbances can alter the distribution of vegetation, bare land, and water bodies.

**Conservation Efforts:** Changes in land cover can also be influenced by conservation and land management efforts. Restoration projects, reforestation, and sustainable land use practices may contribute to shifts in land cover percentages.

**Human Activities:** Human activities, such as agriculture, logging, and mining, can result in changes to land cover. Clearing of forests for agriculture or logging can reduce vegetation cover, while mining activities can lead to alterations in bare land areas.

Table 4.6 provides the percentage distribution of land cover classes across different years. The table presents the percentages of vegetation, built-up areas, bare land, and water bodies for the years 2000, 2010, and 2020, offering insights into the changing composition of land cover over time. This information is complemented by Figure 4.11, which visually presents the trends in land cover class percentages for the specified years

Table 4.6: Showing the percentage of the land cover classes

<b>class</b>	<b>2000</b>	<b>2010</b>	<b>2020</b>
vegetation	53.66%	54.03%	53.69%
built up	7.05%	14.49%	26.57%
bare land	39.26%	31.43%	19.70%
water body	0.03%	0.05%	0.04%

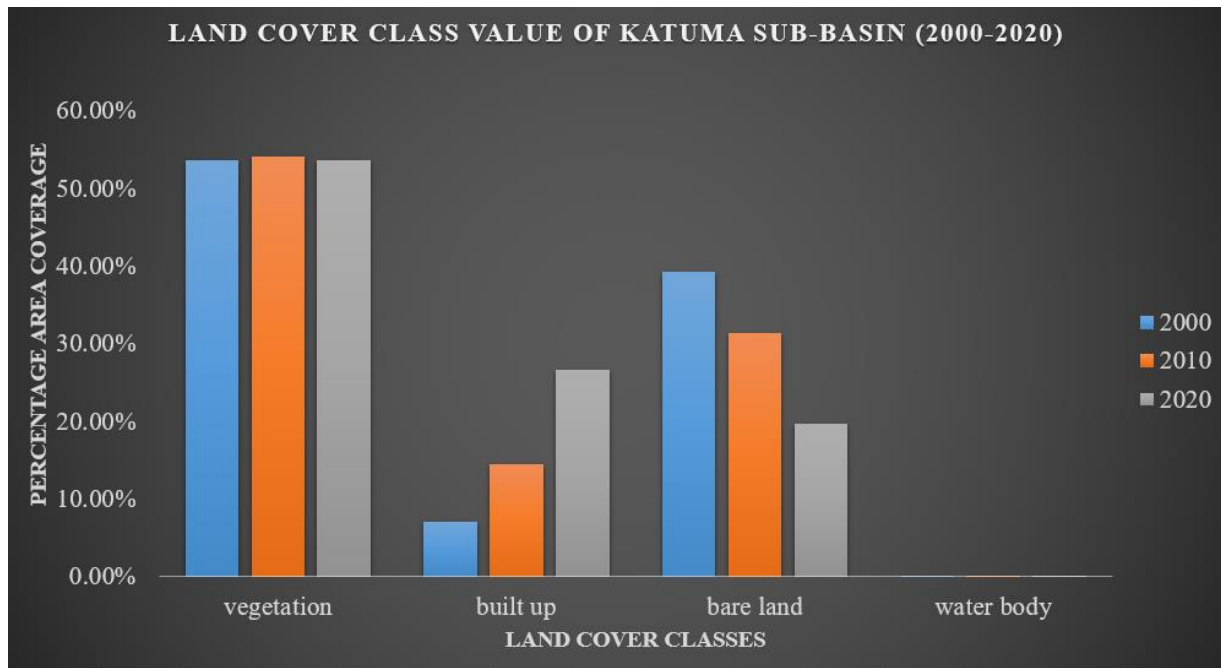


Figure 4.11: Showing the graphical representation of the land cover classes.

#### 4.6.4 Correlation analysis

The correlation was done to all the the datasets used in the analyzing the impact of climate variability on vegetation cover in Katuma sub basin. These datasets include maximum temperature, minimum temperature and rainfall.

Table 4.7 illustrates the relationship between temperature, rainfall, and vegetation cover over the studied years. The table provides data on the percentage of vegetation cover, maximum temperature, minimum temperature, and rainfall for the years 2000, 2010, and 2020. These values offer insights into the variations in vegetation cover in relation to temperature and rainfall patterns

Table 4.7: The relationship between temperature, rainfall and vegetation cover.

year	vegetation	maximum temperature	minimum temperature	rainfall
2000	53.66%	29.54	29.51	1018
2010	54.03%	29.81	29.74	1130
2020	52.69%	29.99	29.95	1048

The correlation values for minimum and maximum temperature over the vegetation cover shows a strong negative correlation. Temperature plays a detrimental effect on the vegetation cover. As for the maximum temperature affects the vegetation growth since extreme heat and

heat stress negatively affect the health and growth of vegetation. Additionally in lower minimum temperature, limit the growth and survival of vegetation especially when the temperature falls below the optimum value for the vegetation to support its growth.

Rainfall shows a positive moderate correlation with vegetation cover. Thus, it signifies that the higher level of rainfall positively influence vegetation cover of the area. Since, sufficient rainfall contributes to the soil moisture availability in which it the man factor in supporting the development and maintain of the vegetation cover.

Table 4.8 displays the correlation values among the datasets analyzed. Specifically, the table presents the correlation values between vegetation cover and the maximum temperature, minimum temperature, and rainfall. The correlation coefficients for these relationships are shown as follows: -0.6164259 for maximum temperature, -0.6847835 for minimum temperature, and 0.5077066 for rainfall.

Table 4.8: Showing the correlation values of the datasets

correlation value		vegetation cover
	max temp	-0.6164259
	min temp	-0.6847835
	rainfall	0.5077066

#### 4.6.5 Land cover change

The changes of land cover from the year 2000 to 2010, 2010 to 2020 and from 2000-2020 were mapped and graphically shown in figure 5.2 to 5.7 respectively. The graphs supports to show which class changed much from one class type to another. The land cover changes observed from the maps and graphs highlight the dynamic nature of the Katuma sub-basin's landscape. The significant increase in built-up areas and the decrease in vegetation cover emphasize the need for sustainable land management practices to mitigate the negative impacts of urbanization and land degradation.

Investigating the dynamics of land cover change, Figure 4.12 provides a visual representation of the shifts observed between 2000 and 2010. This change is further elucidated graphically in Figure 4.13, allowing us to visualize the alterations that took place within this time frame. Similarly, the transition in land cover from 2010 to 2020 is captured in Figure 4.14, while its graphical interpretation can be seen in Figure 4.15. For a comprehensive perspective, the cumulative land cover change over the entire period from 2000 to 2020 is presented in Figure 4.16, with a graphical depiction available in Figure 4.17.

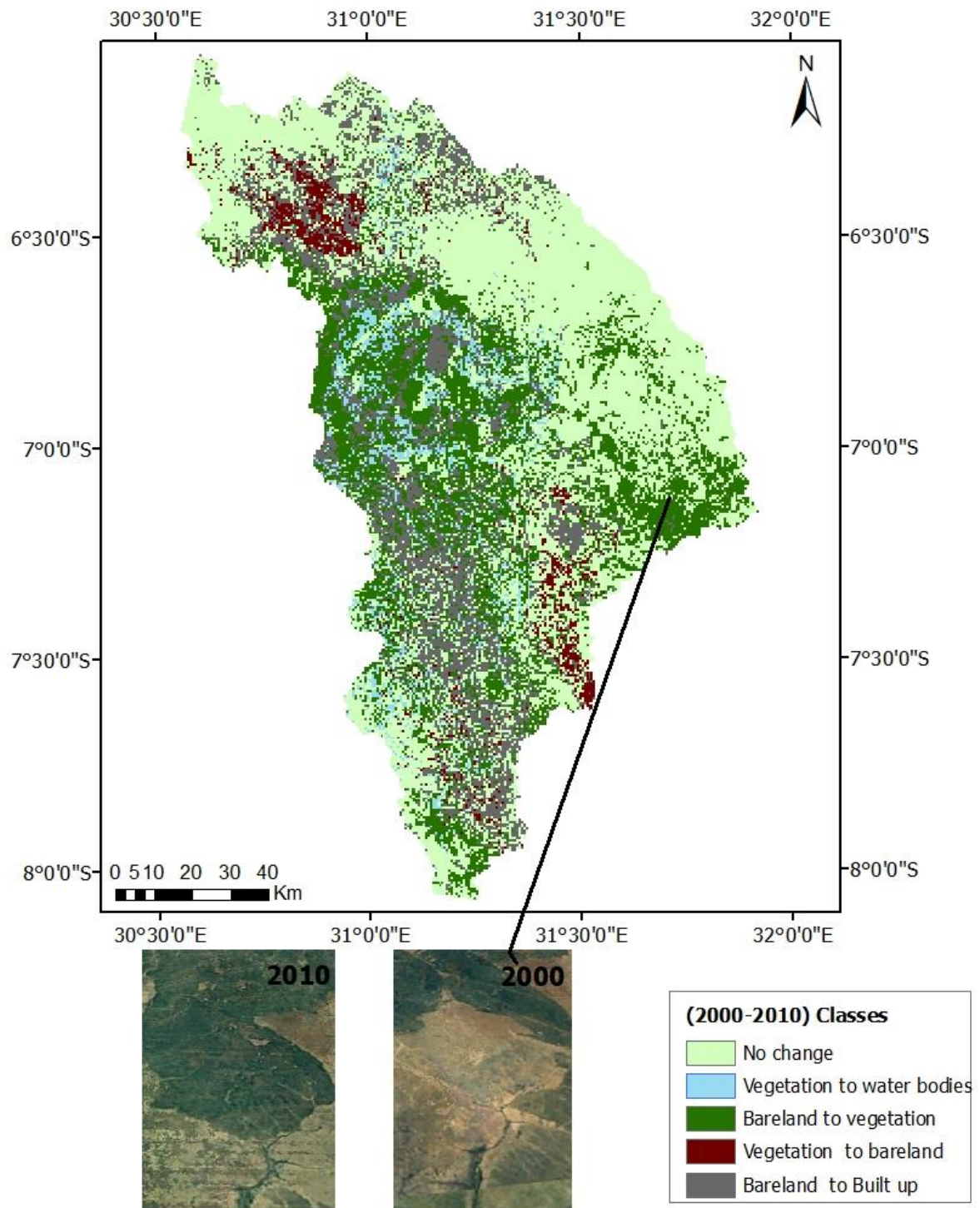


Figure 4.12: Change detection map showing changes in vegetation cover from 2000-2010.



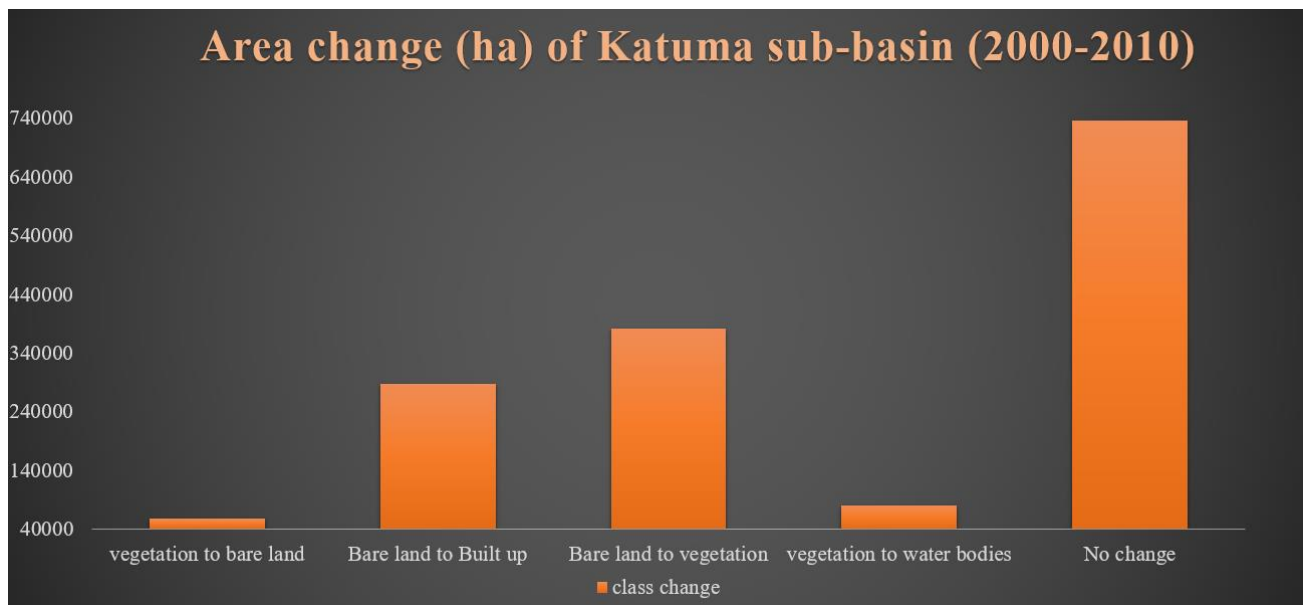


Figure 4.13: graph showing area change of forest cover in Katuma sub basin (2000-2010)

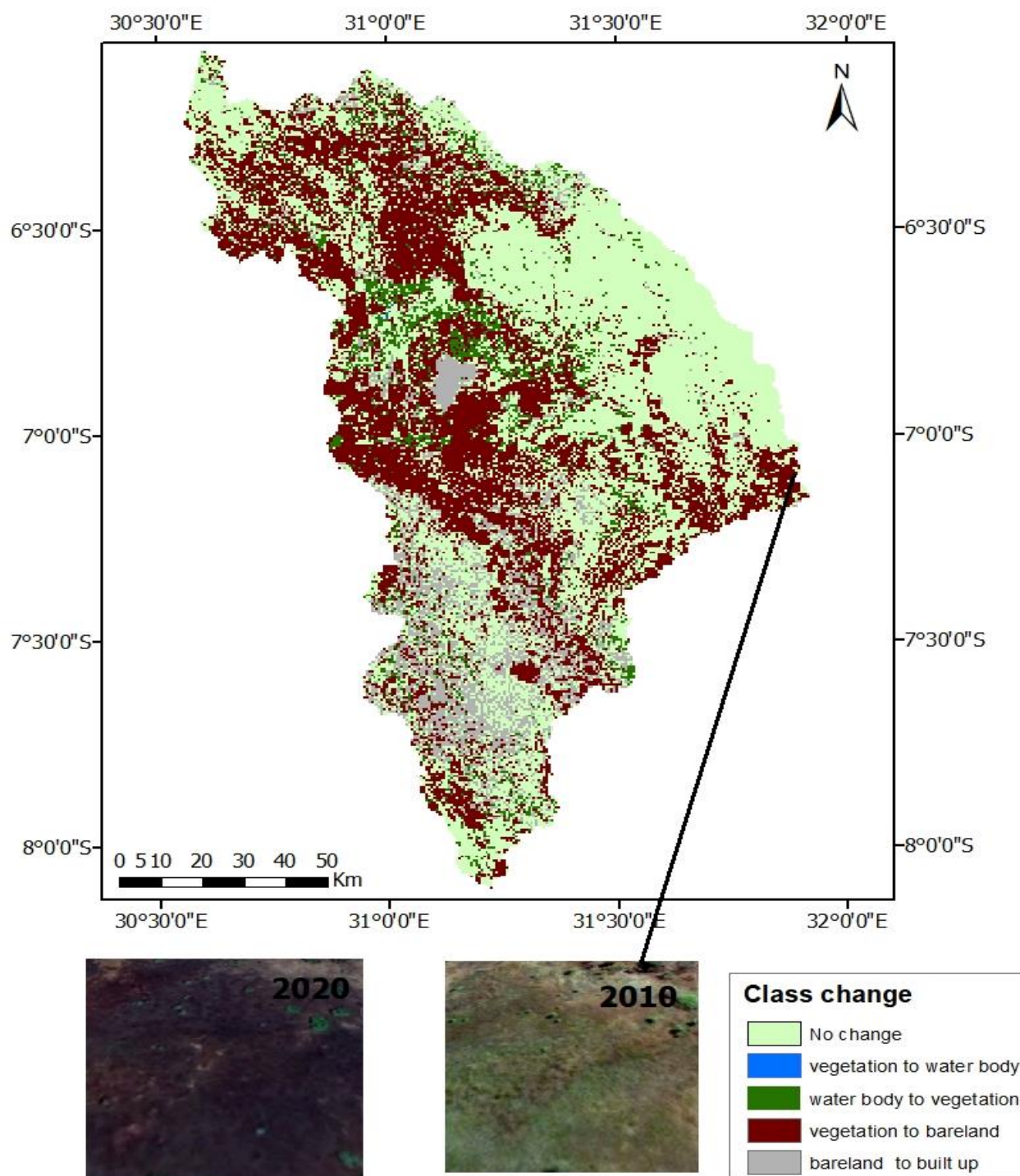


Figure 4.14: Change detection map showing changes in vegetation cover from 2010-2020

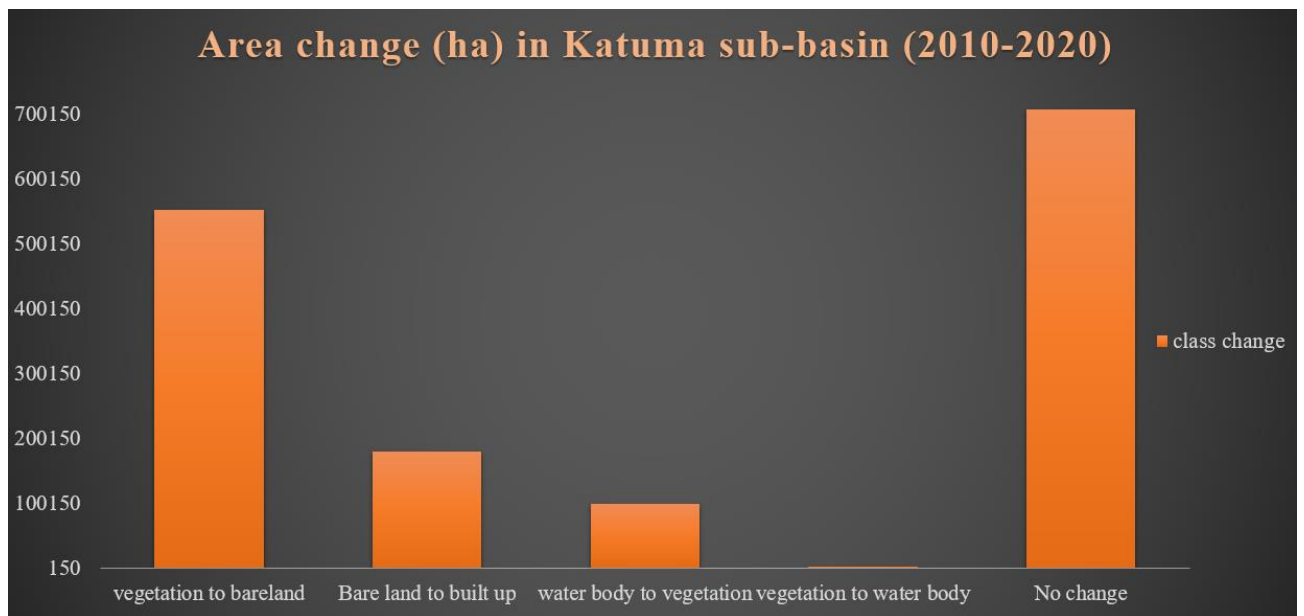


Figure 4.15: Graph showing area change of vegetation cover in Katuma sub basin (2010-2020)

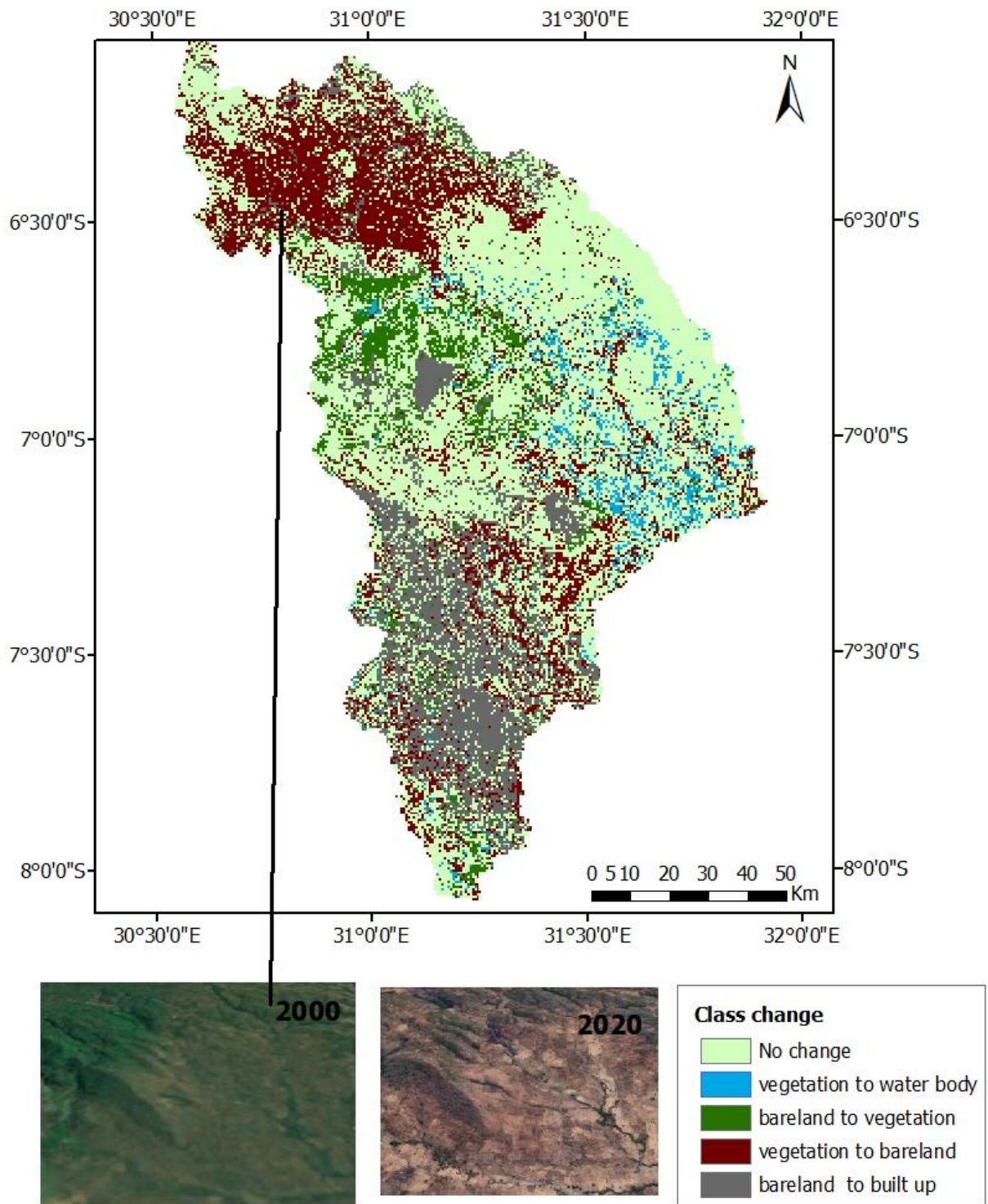


Figure 4.16: change detection map showing change in vegetation cover from 2000-2020

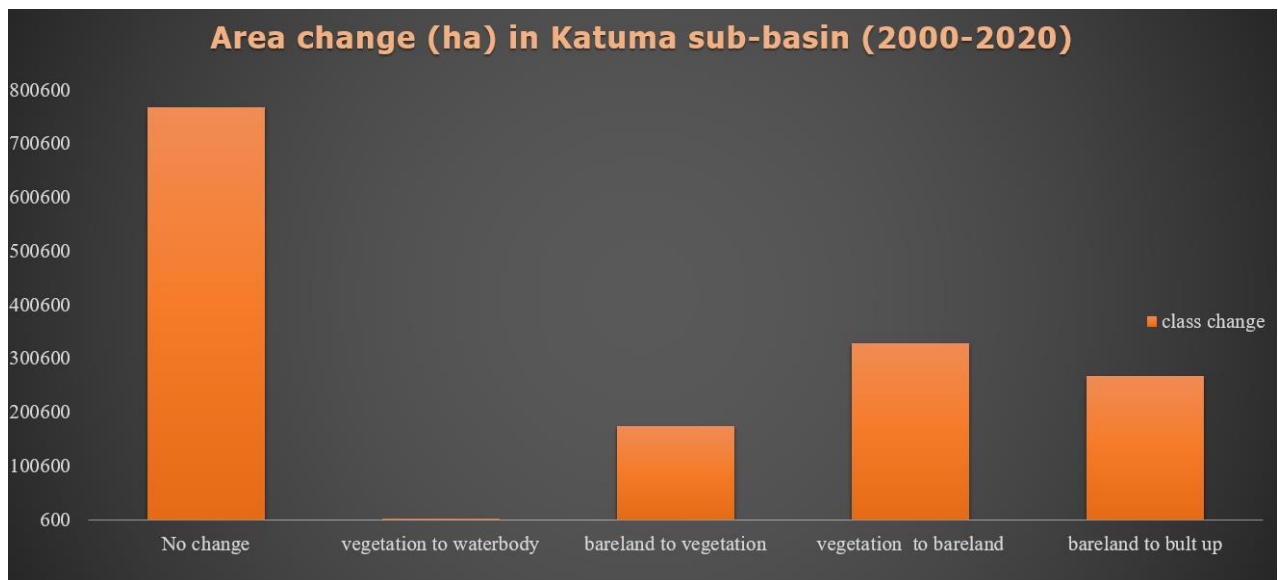


Figure 4.17: Graph showing area change of forest cover in Katuma sub basin (2000-2020)

#### 4.7 Discussion

The analysis of the Normalized Difference Vegetation Index (NDVI) data for the Katuma sub basin from 2000 to 2020 reveals interesting insights into the vegetation health of the region. The NDVI distribution map (Figure 4.1) shows four distinct vegetation classes with varying NDVI values. Overall, there was a significant presence of healthy vegetation, except for a decline in 2007, as indicated by lower NDVI values. The NDVI time series plot (Figure 4.2) depicts the annual distribution of NDVI values, highlighting a peak in 2010, indicating higher vegetation health during those years. The statistical analysis confirms the significance of the NDVI time series, with a positive slope indicating a gradual increase in NDVI values over the study period. The regression equation suggests nourishment in vegetation health within the Katuma sub basin.

In terms of temperature, Figure 4.3 shows a positive slope in both maximum and minimum temperatures, indicating an overall increase from 2000 to 2020. The calculated p-values suggest that these temperature trends are statistically significant. The observed temperature trends align with global climate change patterns, emphasizing the need for monitoring and appropriate measures to mitigate and adapt to the changing climate conditions in the region.

Regarding rainfall, there is a positive trend in annual rainfall variability from 2000 to 2020, as indicated by the slope of the regression equation. The statistically significant p-value reinforces the validity of the observed trend. The increasing trend in annual rainfall has significant

implications for water resources, agriculture, and the overall climate change scenario in the region, requiring adaptive measures and sustainable water management strategies.

The correlation analysis between NDVI and rainfall reveals a positive relationship, indicating that higher rainfall corresponds to increased vegetation health. The significant correlation coefficient and low p-value suggest a true association between these variables.

The land cover analysis using the American Planning Association Land Based Classification Standards (LBCS) provides valuable insights into the distribution and changes in land cover classes in the Katuma sub basin. The accuracy assessment results indicate varying levels of accuracy and reliability for different land cover classes and across different years.

The quantification of land cover classes shows significant changes over the period of 2000-2020. Built-up areas have increased, while vegetation cover has fluctuated; influenced by factors such as climate variability, land management practices, and natural disturbances. These changes have implications for water resources, ecosystems, and human activities, necessitating sustainable land management practices.

The correlation analysis between temperature, rainfall, and vegetation cover reveals a negative correlation between temperature (both maximum and minimum) and vegetation cover, while rainfall shows a positive moderate correlation. Extreme heat and lower temperatures negatively affect vegetation health, while sufficient rainfall supports vegetation growth.

The land cover change maps and graphs highlight the dynamic nature of the Katuma sub-basin's landscape, with a significant increase in built-up areas and a decrease in vegetation cover

## CHAPTER FIVE

### CONCLUSION AND RECOMMENDATION

#### 5.1 Conclusion

The analysis of climate variability and its impact on vegetation cover in the Katuma sub-basin has yielded valuable insights into the complex interplay between environmental factors. Through an in-depth examination of earth observation data spanning from 2000 to 2020, this study has shed light on how changes in temperature, rainfall, and land cover influence vegetation health and distribution.

The study's findings indicate a positive trend in vegetation health over the years, as reflected by the NDVI time series trend of 0.00033 (not statistically significant at  $p = 0.47$ ). While the trends in temperature exhibited an overall increase, with a positive trend of 0.01109 for maximum temperature and 0.01323 for minimum temperature (both statistically significant at  $p = 0.00201$  and  $p = 0.0497$ , respectively), the correlation analyses uncovered intricate relationships between these climatic variables and vegetation cover. A positive correlation of 0.68 between NDVI and precipitation was observed, suggesting that vegetation health is influenced by the availability of water. However, negative correlations were found between vegetation cover and temperature, with values of -0.6164 for minimum temperature and -0.6847 for maximum temperature, and a positive correlation of 0.5077 between vegetation cover and precipitation.

The examination of land cover changes using land cover maps revealed significant shifts in the proportions of different land cover classes, indicating the ongoing dynamics of urbanization, land use, and natural processes within the sub-basin. The spatial distribution of vegetation cover exhibited fluctuations, emphasizing the importance of considering both temporal and spatial dimensions in understanding how vegetation responds to changing environmental conditions.

In light of these findings, it is evident that climate variability exerts a multifaceted influence on the vegetation dynamics of the Katuma sub-basin. The study underscores the importance of adopting a comprehensive approach that takes into account not only the climate variables but also the intricate interactions between land cover changes, human activities, and ecological processes.

These insights have broader implications for land management, conservation strategies, and policy decisions aimed at maintaining and enhancing vegetation health in the face of a



changing climate. By recognizing the intricate relationships between climate variability, land cover changes, and vegetation health, stakeholders can make informed choices to ensure the sustainable management of the Katuma sub-basin's ecosystems.

In summary, this research has fulfilled its main objective of analyzing the impact of climate variability on vegetation cover in the Katuma sub-basin. The study's specific objectives of assessing land cover dynamics, quantifying temperature and rainfall trends, and investigating correlations between NDVI and climatic variables have all contributed to a deeper understanding of the interactions between climate and vegetation dynamics. These findings provide a valuable foundation for guiding future land management and conservation efforts in the region.

## **5.2 Recommendation**

This study recommends expanding the scope of analysis beyond temperature and rainfall to encompass the influence of anthropogenic activities. To enhance the accuracy of data analysis, it is advisable to leverage advanced statistical techniques and cutting-edge remote sensing technologies. Employing data fusion methods can further enhance the depth of understanding. Additionally, the findings of this research emphasize the significance of conducting comparative studies across various sub-basins and basins. Such comparative analyses can validate the observed patterns and uncover common trends. As a result, it is imperative to conduct further investigations that encompass a broader range of factors affecting vegetation cover in different sub-basins and basins as a whole. This will contribute to a more comprehensive understanding of the complex interplay between climate variability and vegetation dynamics.



## REFERENCE

- Agrawala, S., Moehner, A., Hemp, A., & Al, E. (2003). Development and climate change in Tanzania: focus on Mount Kilimanjaro *and Development* 72 pp. <http://www.oecd.org/dataoecd/47/0/21058838.pdf>
- Avtar, R., Komolafe, A. A., Kouser, A., Singh, D., Yunus, A. P., Dou, J., Kumar, P., Gupta, R. Das, Johnson, B. A., & Minh, H. V. T. (2020). Assessing sustainable development prospects through remote sensing: A review. *Remote Sensing Applications: Society and Environment*, 20, 100402.
- Campbell, J. B., & Wynne, R. H. (2011a). *Introduction to Remote Sensing, Fifth Edition*. Guilford Press.
- Campbell, J. B., & Wynne, R. H. (2011b). *Introduction to remote sensing*. Guilford Press.
- Canty, M. J. (2014). *Image Analysis, Classification and Change Detection in Remote Sensing: With Algorithms for ENVI/IDL and Python, Third Edition*. CRC Press. <https://books.google.co.tz/books?id=fGDOBQAAQBAJ>
- Cloern, J. E., Abreu, P. C., Carstensen, J., Chauvaud, L., Elmgren, R., Grall, J., Greening, H., Johansson, J. O. R., Kahru, M., Sherwood, E. T., Xu, J., & Yin, K. (2016). Human activities and climate variability drive fast-paced change across the world's estuarine-coastal ecosystems. *Global Change Biology*, 22(2), 513–529. <https://doi.org/10.1111/gcb.13059>
- Correlation (Pearson, Kendall, Spearman) - Statistics Solutions*. (2023). <https://www.statisticssolutions.com/free-resources/directory-of-statistical-analyses/correlation-pearson-kendall-spearman/>
- Detto, M., Wright, S. J., Calderón, O., & Muller-Landau, H. C. (2018). Resource acquisition and reproductive strategies of tropical forest in response to the El Niño–Southern Oscillation. *Nature Communications*, 9(1), 913.
- Fischer, M. M., & Getis, A. (2010). *Handbook of applied spatial analysis: software tools, methods and applications*. Springer. <http://files/50/Fischer and Getis - 2010 - Handbook of applied spatial analysis software too.pdf>
- Internationa, W. (2016). *Lake Rukwa Basin Integrated Water Resources Management and*

- Development Plan, Final Report, Volume VI: Lake Rukwa Basin Monitoring Plan. Technical.* WREM International Inc. <https://studylib.net/doc/9522728/1.2-background-information-about-lake-rukwa-basin>
- Jensen, J. R. (2015). *Introductory Digital Image Processing: A Remote Sensing Perspective.* Pearson Education. <https://books.google.co.tz/books?id=BWx3CgAAQBAJ>
- Konecny, G. (2014). *Geoinformation: Remote Sensing, Photogrammetry and Geographic Information Systems, Second Edition.* CRC Press. <https://books.google.co.tz/books?id=8TcyAwAAQBAJ>
- Leweri, C. M., Msuha, M. J., & Treydte, A. C. (2021). Rainfall variability and socio-economic constraints on livestock production in the Ngorongoro Conservation Area, Tanzania. *SN Applied Sciences*, 3(1), 1–10. <https://doi.org/10.1007/s42452-020-04111-0>
- Liang, Y., Liu, L., Huang, J., Liang, Y., Liu, L., & Huang, J. (2020). Vegetation change detection using trend analysis and remote sensing. *Integrated Modelling of Ecosystem Services and Land-Use Change: Case Studies of Northwestern Region of China*, 39–57.
- Mann, H. B. (1945). Nonparametric tests against trend. *Econometrica: Journal of the Econometric Society*, 245–259.
- Mbonile, M. J. (2005). Migration and intensification of water conflicts in the Pangani Basin, Tanzania. *Habitat International*, 29(1), 41–67. [https://doi.org/10.1016/S0197-3975\(03\)00061-4](https://doi.org/10.1016/S0197-3975(03)00061-4)
- Mnaya, B., Elisa, M., Kihwele, E., Kiwango, H., Kiwango, Y., Ng’umbi, G., & Wolanski, E. (2021). Are Tanzanian National Parks affected by the water crisis? Findings and ecohydrology solutions. *Ecohydrology & Hydrobiology*, 21(3), 425–442. <https://doi.org/10.1016/j.ecohyd.2021.04.003>
- Munishi, P. K. T., Temu, R.-A. P. C., & Soka, G. (2011). *Plant communities and tree species associations in a Miombo ecosystem in the Lake Rukwa basin, Southern Tanzania: implications for conservation.* <http://www.suaire.sua.ac.tz/handle/123456789/4199>
- Rouse, J. W., Haas, R. H., Schell, J. A., & Deering, D. W. (1974). Monitoring vegetation systems in the Great Plains with ERTS. *NASA Spec. Publ*, 351(1), 309.
- Satellite imagery. (2023). In *Wikipedia*. [https://en.wikipedia.org/w/index.php?title=Satellite\\_imagery&oldid=1142730516](https://en.wikipedia.org/w/index.php?title=Satellite_imagery&oldid=1142730516)

- Seeteram, N. A., Hyera, P. T., Kaaya, L. T., Lalika, M. C. S., & Anderson, E. P. (2019). Conserving rivers and their biodiversity in Tanzania. *Water*, 11(12), 2612.
- The International Union for Conservation of Nature (IUCN). (2017, April 23). SUSTAIN's interest-driven partnerships: a win-win for river flow and farmers' fields. *IUCN*. <https://www.iucn.org/news/water/201711/sustain's-interest-driven-partnerships-win-win-river-flow-and-farmers'-fields>
- Tzanakakis, V. A. (2020). Water | Free Full-Text | Water Supply and Water Scarcity. *Water*, 12(2347). <https://doi.org/10.3390/w12092347>
- Vermote, E. F., Roger, J. C., & Ray, J. P. (2015). MODIS surface reflectance user's guide [R/OL]. *MODIS Land Surface Reflectance Science Computing Facility*.
- Wan, Z., Zhang, Y., Zhang, Q., & Li, Z.-L. (2004). Quality assessment and validation of the MODIS global land surface temperature. *International Journal of Remote Sensing*, 25(1), 261–274.
- Wang, F., Shao, W., Yu, H., Kan, G., He, X., Zhang, D., Ren, M., & Wang, G. (2020). Re-evaluation of the power of the mann-kendall test for detecting monotonic trends in hydrometeorological time series. *Frontiers in Earth Science*, 8, 14.
- Wu, Z., Jiang, Q., Yu, Y., Xiao, H., & Freese, D. (2022). Spatio-Temporal Evolution of a Typical Sandstorm Event in an Arid Area of Northwest China in April 2018 Based on Remote Sensing Data. *Remote Sensing*, 14(13), 3065.
- Xu, C., Gorum, T., & Tanyas, H. (2022). *Application of Remote Sensing and GIS in Earthquake-Triggered Landslides*. Frontiers Media SA. <https://www.google.co.tz/books?id=hvSDEAAAQBAJ>
- Zhang, Y., Li, H., & Reggiani, P. (2019). *Climate variability and climate change impacts on land surface, hydrological processes and water management* (Vol. 11). MDPI.